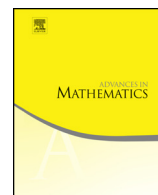




Contents lists available at ScienceDirect

Advances in Mathematics

www.elsevier.com/locate/aim

Tropicalization of del Pezzo surfaces

Qingchun Ren^a, Kristin Shaw^b, Bernd Sturmfels^{c,*}^a Google Inc, Mountain View, CA 94043, USA^b Technische Universität Berlin, MA 6-2, 10623 Berlin, Germany^c University of California, Berkeley, CA 94720-3840, USA

ARTICLE INFO

Article history:

Received 25 February 2014

Accepted 4 March 2015

Available online 30 March 2016

Keywords:

Tropical geometry

Cubic surface

Cox ring

27 lines

Tropical modification

Tropical basis

Hyperplane arrangement

Weyl group

Polyhedral fan

ABSTRACT

We determine the tropicalizations of very affine surfaces over a valued field that are obtained from del Pezzo surfaces of degree 5, 4 and 3 by removing their (-1) -curves. On these tropical surfaces, the boundary divisors are represented by trees at infinity. These trees are glued together according to the Petersen, Clebsch and Schläfli graphs, respectively. There are 27 trees on each tropical cubic surface, attached to a bounded complex with up to 73 polygons. The maximal cones in the 4-dimensional moduli fan reveal two generic types of such surfaces.

© 2016 Published by Elsevier Inc.

1. Introduction

A smooth cubic surface X in projective 3-space \mathbb{P}^3 contains 27 lines. These lines are characterized intrinsically as the (-1) -curves on X , that is, rational curves of self-intersection -1 . The tropicalization of an embedded surface X is obtained directly from the cubic polynomial that defines it in \mathbb{P}^3 . The resulting tropical surfaces are dual to

* Corresponding author.

E-mail addresses: qingchun.ren@gmail.com (Q. Ren), shaw@math.tu-berlin.de (K. Shaw), bernd@berkeley.edu (B. Sturmfels).

regular subdivisions of the size 3 tetrahedron. These come in many combinatorial types [15, §4.5]. If the subdivision is a unimodular triangulation then the tropical surface is called smooth (cf. [15, Prop. 4.5.1]).

Alternatively, by removing the 27 lines from the cubic surface X , we obtain a very affine surface X^0 . In this paper, we study the tropicalization of X^0 , denoted $\text{trop}(X^0)$, via the embedding in its intrinsic torus [11]. This is an invariant of the surface X . The (-1) -curves on X now become visible as 27 *boundary trees* on $\text{trop}(X^0)$. This distinguishes our approach from Vigeland’s work [27] on the 27 lines on tropical cubics in \mathbb{TP}^3 . It also highlights an important feature of tropical geometry [17]: there are different tropical models of a single classical variety, and the choice of model depends on what structure one wants revealed.

Throughout this paper we work over a field K of characteristic zero that has a non-archimedean valuation. Examples include the Puiseux series $K = \mathbb{C}\{\{t\}\}$ and the p -adic numbers $K = \mathbb{Q}_p$. We use the term *cubic surface* to mean a marked smooth del Pezzo surface X of degree 3. A *tropical cubic surface* is the intrinsic tropicalization $\text{trop}(X^0)$ described above. Likewise, *tropical del Pezzo surface* refers to the tropicalization $\text{trop}(X^0)$ for degree ≥ 4 . Here, the adjective “tropical” is used solely for brevity, instead of the more accurate “tropicalized” used in [15]. We do not consider non-realizable tropical del Pezzo surfaces, nor tropicalizations of surfaces defined over a field K with positive characteristic.

The moduli space of cubic surfaces is four-dimensional, and its tropical version is the four-dimensional *Naruki fan*. This was constructed combinatorially by Hacking, Keel and Tevelev [11], and it was realized in [20, §6] as the tropicalization of a very affine variety \mathcal{Y}^0 , obtained from the Yoshida variety \mathcal{Y} in \mathbb{P}^{39} by intersecting with $(K^*)^{39}$. The Weyl group $W(E_6)$ acts on \mathcal{Y} by permuting the 40 coordinates. The maximal cones in $\text{trop}(\mathcal{Y}^0)$ come in two $W(E_6)$ -orbits. We here compute the corresponding cubic surfaces:

Theorem 1.1. *There are two generic types of tropical cubic surfaces. They are contractible and characterized at infinity by 27 metric trees, each having 10 leaves. The first type has 73 bounded cells, 150 edges, 78 vertices, 135 cones, 189 flaps, 216 rays, and all 27 trees are trivalent. The second type has 72 bounded cells, 148 edges, 77 vertices, 135 cones, 186 flaps, 213 rays, and three of the 27 trees have a 4-valent node. (For more data see Table 1.)*

Here, by *cones* and *flaps* we mean unbounded 2-dimensional polyhedra that are affinely isomorphic to $\mathbb{R}_{\geq 0}^2$ and $[0, 1] \times \mathbb{R}_{\geq 0}$ respectively. The *characterization at infinity* is analogous to that for tropical planes in [12]. Indeed, by [12, Theorem 4.4], every tropical plane L in \mathbb{TP}^{n-1} is given by an arrangement of n boundary trees, each having $n - 1$ leaves, and L is uniquely determined by this arrangement. Viewed intrinsically, L is the tropicalization of a very affine surface, namely the complement of n lines in \mathbb{P}^2 . Theorem 1.1 offers the analogous characterization for the tropicalization of the complement of the 27 lines on a cubic surface.

Tropical geometry has undergone an explosive development during the past decade. To the outside observer, the literature is full of conflicting definitions and diverging approaches. The text books [15,17] offer some help, but they each stress one particular point of view.

An important feature of the present paper is its focus on the unity of tropical geometry. We shall develop three different techniques for computing tropical del Pezzo surfaces:

- Cox ideals, as explained in Section 2;
- fan structures on moduli spaces, as explained in Section 3;
- tropical modifications, as explained in Section 4.

The first approach uses the Cox ring of X , starting from the presentation given in [26]. Propositions 2.1 and 2.2 extend this to the universal Cox ideal over the moduli space. For any particular surface X , defined over a field such as $K = \mathbb{Q}(t)$, computing the tropicalization is a task for the software `gfan` [13]. In the second approach, we construct del Pezzo surfaces from fibers in the natural maps of moduli fans. Our success along these lines completes the program started by Hacking et al. [11] and further developed in [20, §6]. The third approach is to build tropical del Pezzo surfaces combinatorially from the tropical projective plane \mathbb{TP}^2 by the process of tropical modifications in the sense of Mikhalkin [16]. It mirrors the classical construction by blowing up points in \mathbb{P}^2 . All three approaches yield the same results. Section 5 presents an in-depth study of the combinatorics of tropical cubic surfaces and their trees, including an extension of Theorem 1.1 that includes all degenerate surfaces.

We now illustrate the rich combinatorics in our story for a del Pezzo surface X of degree 4. Del Pezzo surfaces of degree $d \geq 6$ are toric surfaces, so they naturally tropicalize as polygons with $12 - d$ vertices [17, Ch. 3]. On route to Theorem 1.1, we prove the following for $d = 4, 5$:

Proposition 1.2. *Among tropical del Pezzo surfaces of degree 4 and 5, each has a unique generic combinatorial type. For degree 5, this is the cone over the Petersen graph. For degree 4, the surface is contractible and characterized at infinity by 16 trivalent metric trees, each with 5 leaves. It has 9 bounded cells, 20 edges, 12 vertices, 40 cones, 32 flaps, and 48 rays.*

To understand degree 4, we consider the 5-regular *Clebsch graph* in Fig. 1. Its 16 nodes are the (-1) -curves on X , labeled $E_1, \dots, E_5, F_{12}, \dots, F_{45}, G$. Edges represent intersecting pairs of (-1) -curves. In the constant coefficient case, when K has trivial valuation, the tropicalization of X is the fan over this graph. However, over fields K with non-trivial valuation, $\text{trop}(X^0)$ is usually not a fan, but one sees the generic type from Proposition 1.2. Here, the Clebsch graph deforms into a trivalent graph with $48 = 16 \cdot 3$ nodes and $72 = 40 + 32$ edges, determined by the color coding in Fig. 1. Each of the 16 nodes is replaced by a trivalent tree with five leaves. Incoming edges of the same color

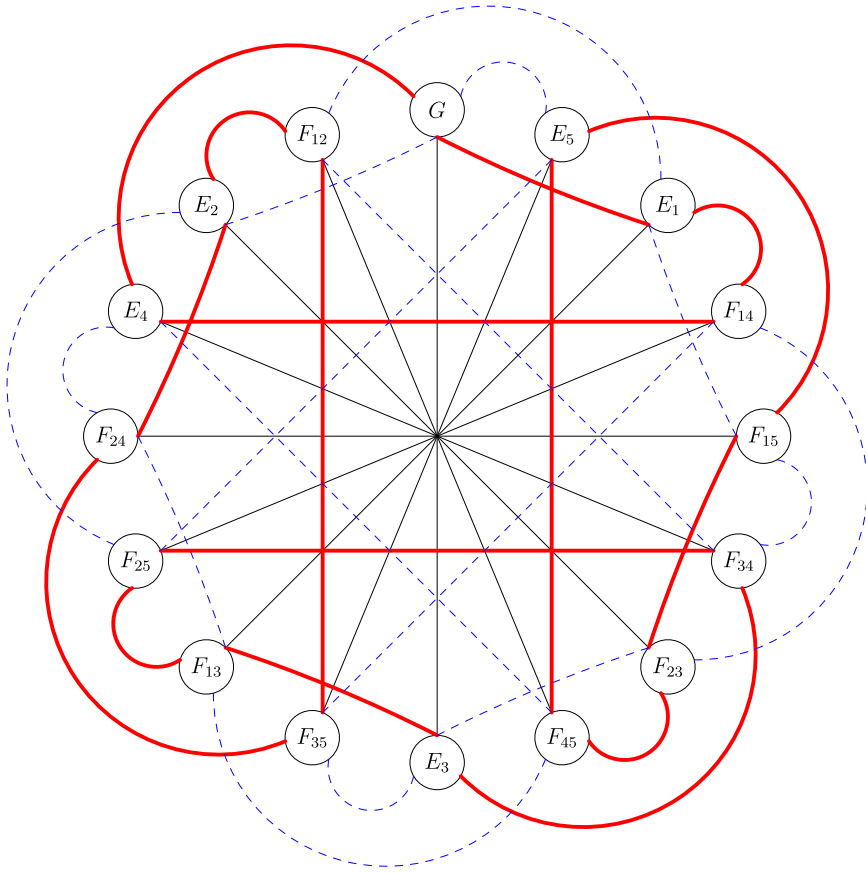


Fig. 1. Tropical del Pezzo surfaces of degree 4 illustrated by marking the edges of the Clebsch graph. (For interpretation of the references to color in this figure, the reader is referred to the web version of this article.)

(red or blue) form a *cherry* (= two adjacent leaves) in that tree, while the black edge connects to the non-cherry leaf.

Corollary 1.3. *For a del Pezzo surface X of degree 4, the 16 metric trees on its tropicalization $\text{trop}(X^0)$, obtained from the (-1) -curves on X , are identical up to relabeling.*

Proof. Moving from one (-1) -curve on X to another corresponds to a Cremona transformation of the plane \mathbb{P}^2 . Each (-1) -curve on X has exactly five marked points arising from its intersections with the other (-1) -curves. Moreover, the Cremona transformations preserve the cross ratios among the five marked points on these 16 \mathbb{P}^1 's. From the valuations of all the various cross ratios one can read off the combinatorial trees along with their edge lengths, as explained in e.g. [15, Proposition 6.5.1] or [20, Example 5.2]. We then obtain the following relabeling rules for the leaves on the 16 trees, which live in the circular nodes of Fig. 1.

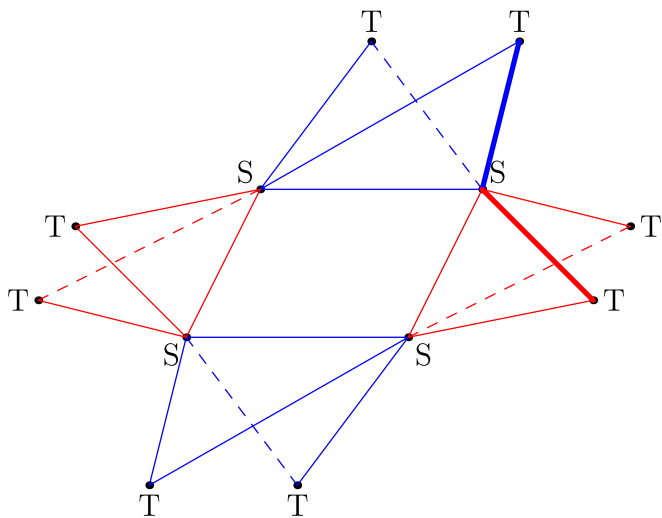


Fig. 2. The bounded complex of the tropical del Pezzo surface in degree 4. (For interpretation of the references to color in this figure, the reader is referred to the web version of this article.)

We start with the tree G whose leaves are labeled E_1, E_2, E_3, E_4, E_5 . For the specific example in Fig. 1, this is the caterpillar tree $(\{E_1, E_4\}, E_3, \{E_2, E_5\})$. Now, given any trivalent tree for G , the tree F_{ij} is obtained by relabeling the five leaves as follows:

$$E_i \mapsto E_j, \quad E_j \mapsto E_i, \quad E_k \mapsto F_{lm}, \quad E_l \mapsto F_{km}, \quad E_m \mapsto F_{kl}. \tag{1.1}$$

Here $\{k, l, m\} = \{1, 2, 3, 4, 5\} \setminus \{i, j\}$. The tree E_i is obtained from the tree G by relabeling

$$E_i \mapsto G \quad \text{and} \quad E_j \mapsto F_{ij} \quad \text{where } j \neq i. \tag{1.2}$$

This explains the color coding of the graph in Fig. 1. \square

The bounded complex of $\text{trop}(X^0)$ is shown in Fig. 2. It consists of a central rectangle, with two triangles attached to each of its four edges. There are 12 vertices, four vertices of the rectangle, labeled **S**, and eight pendant vertices, labeled **T**. To these 12 vertices and 20 edges, we attach the flaps and cones, according to the deformed Clebsch graph structure. The link of each **S** vertex in the surface $\text{trop}(X^0)$ is the Petersen graph (Fig. 3), while the link of each **T** vertex is the bipartite graph $K_{3,3}$. The bounded complex has 16 chains **TST** consisting of two edges with different colors. These are attached by flaps to the bounded parts of the 16 trees. The Clebsch graph (Fig. 1) can be recovered from Fig. 2 as follows: its nodes are the **TST** chains, and two chains connect if they share precisely one vertex. Out at infinity, **T** vertices attach along cherries, while **S** vertices attach along non-cherry leaves. Each such attachment between two of the 16 trees links to the bounded complex by a cone.

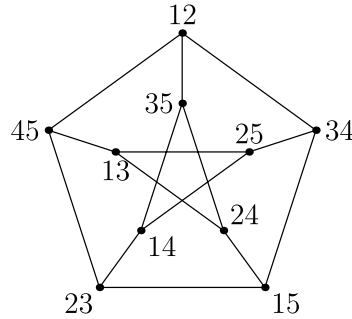


Fig. 3. The tropical del Pezzo surface $\text{trop}(M_{0,5})$ is the cone over the Petersen graph.

2. Cox ideals

We study del Pezzo surfaces over K of degrees 5, 4 and 3. Such surfaces X are obtained from \mathbb{P}^2 by blowing up 4, 5 or 6 points in general position, and we obtain moduli by varying these points. From an algebraic perspective, it is convenient to represent X by its *Cox ring*

$$\text{Cox}(X) = \bigoplus_{\mathcal{L} \in \text{Pic}(X)} H^0(X, \mathcal{L}). \quad (2.1)$$

The Cox ring of a del Pezzo surface X was first studied by Batyrev and Popov [4]. We shall express this ring explicitly as a quotient of a polynomial ring over the ground field K :

$$\text{Cox}(X) = K[x_C : C \text{ is a } (-1)\text{-curve on } X] \text{ modulo an ideal } I_X \text{ generated by quadrics.}$$

The number of variables x_C in our three polynomial rings is 10, 16 and 27 respectively. The ideal I_X is the *Cox ideal* of the surface X . It was conjectured already in [4] that the ideal I_X is generated by quadrics. This conjecture was proved in several papers, including [25,26].

The Cox ring encodes all maps from X to a projective space. Such a map is given by the \mathbb{N} -graded subring $\text{Cox}(X)_{[\mathcal{L}]} = \bigoplus_{m \geq 0} H^0(X, m\mathcal{L})$ for a fixed line bundle $\mathcal{L} \in \text{Pic}(X)$. The image of the map $X \rightarrow \text{Proj}(\text{Cox}(X)_{[\mathcal{L}]})$ is contained in the projective space \mathbb{P}^N , where $N = \dim(H^0(X, \mathcal{L})) - 1$, provided $\text{Cox}(X)_{[\mathcal{L}]}$ is generated in degree 1. This applies to both the anticanonical map and to the blow-down map to \mathbb{P}^2 .

In what follows, we give explicit generators for all relevant Cox ideals I_X . Some of this is new and of independent interest. The tropicalization of X^0 we seek is defined from the ideal I_X . So, in principle, we can compute $\text{trop}(X^0)$ from I_X using the software **gfan** [13]. Recall that X^0 denotes the very affine surface obtained from X by removing all (-1) -curves.

Del Pezzo surfaces of degree 5

Consider four general points in \mathbb{P}^2 . This configuration is projectively unique, so there are no moduli. The surface X is the moduli space $\overline{M}_{0,5}$ of rational stable curves with five marked points, see for example [14]. The very affine variety X^0 is simply $M_{0,5}$, the moduli space of rational curves with five distinct marked points. It is the complement of a hyperplane arrangement whose underlying matroid is the graphical matroid of the complete graph K_4 . The Cox ideal is the *Plücker ideal* of relations among 2×2 -minors of a 2×5 -matrix:

$$I_X = \langle p_{12}p_{34} - p_{13}p_{24} + p_{14}p_{23}, \quad p_{12}p_{35} - p_{13}p_{25} + p_{15}p_{23}, \\ p_{12}p_{45} - p_{14}p_{25} + p_{15}p_{24}, \quad p_{13}p_{45} - p_{14}p_{35} + p_{15}p_{34}, \quad p_{23}p_{45} - p_{24}p_{35} + p_{25}p_{34} \rangle.$$

The affine variety of I_X in \bar{K}^{10} is the *universal torsor* of X , now regarded over the algebraic closure \bar{K} of the given valued field K . From the perspective of blowing up \mathbb{P}^2 at 4 points, the ten variables (representing the ten (-1) -curves) fall in two groups: the four exceptional fibers, and the six lines spanned by pairs of points. For example, we may label the fibers by

$$E_1 = p_{15}, \quad E_2 = p_{25}, \quad E_3 = p_{35}, \quad E_4 = p_{45},$$

and the six lines by

$$F_{12} = p_{34}, \quad F_{13} = p_{24}, \quad F_{14} = p_{23}, \quad F_{23} = p_{14}, \quad F_{24} = p_{13}, \quad F_{34} = p_{12}.$$

The Cox ideal I_X is homogeneous with respect to the natural grading by the Picard group $\text{Pic}(X) = \mathbb{Z}^5$. In Plücker coordinates, this grading is given by setting $\deg(p_{ij}) = e_i + e_j$, where e_i represents the i -th standard basis vector in $\mathbb{Z}^5 = \text{Pic}(X)$. This translates into an action of the torus $(\bar{K}^*)^5 = \text{Pic}(X) \otimes_{\mathbb{Z}} \bar{K}^*$ on the universal torsor in \bar{K}^{10} . We remove the ten coordinate hyperplanes in \bar{K}^{10} , and we take the quotient modulo $(\bar{K}^*)^5$. The result is precisely the very affine del Pezzo surface we seek to tropicalize:

$$X^0 = M_{0,5} \subset (\bar{K}^*)^{10}/(\bar{K}^*)^5. \quad (2.2)$$

The 2-dimensional balanced fan $\text{trop}(X^0)$ is the Bergman fan of the graphical matroid of K_4 . It is known from [2] that this is the cone over the Petersen graph. This is also easy to check directly with **gfan** on I_X . This fan is also the moduli space of 5-marked rational tropical curves, that is, 5-leaf trees with lengths on the two bounded edges (cf. [15, §4.3]).

Del Pezzo surfaces of degree 4

Consider now five general points in \mathbb{P}^2 . There are two degrees of freedom. The moduli space is our previous del Pezzo surface $M_{0,5}$. Indeed, fixing five points in \mathbb{P}^2 corresponds to fixing a point (p_{12}, \dots, p_{45}) in $M_{0,5}$, using Cox–Plücker coordinates as in (2.2). Explicitly, if we write the five points as a 3×5 -matrix then the p_{ij} are the Plücker coordinates

of its kernel. Replacing K with the previous Cox ring, we may consider the *universal del Pezzo surface* \mathcal{Y} . The *universal Cox ring* is the quotient of a polynomial ring in $26 = 10 + 16$ variables:

$$K[\mathcal{Y}] = \text{Cox}(M_{0,5})[E_1, E_2, E_3, E_4, E_5, F_{12}, F_{13}, \dots, F_{45}, G]/I_{\mathcal{Y}}. \quad (2.3)$$

As before, E_i represents the exceptional divisor over point i , and F_{ij} represents the line spanned by points i and j . The variable G represents the conic spanned by the five points.

Proposition 2.1. *Up to saturation with respect to the product of the 26 variables, the universal Cox ideal $I_{\mathcal{Y}}$ for degree 4 del Pezzo surfaces is generated by the following 45 trinomials:*

<i>Base Group</i>	$p_{12}p_{34} - p_{13}p_{24} + p_{14}p_{23}$	$p_{12}p_{35} - p_{13}p_{25} + p_{15}p_{23}$	$p_{12}p_{45} - p_{14}p_{25} + p_{15}p_{24},$
	$p_{13}p_{45} - p_{14}p_{35} + p_{15}p_{34}$	$p_{23}p_{45} - p_{24}p_{35} + p_{25}p_{34}$	
<i>Group 1</i>	$F_{23}F_{45} - F_{24}F_{35} + F_{25}F_{34}$	$p_{23}p_{45}F_{24}F_{35} - p_{24}p_{35}F_{23}F_{45} - GE_1$	
	$p_{23}p_{45}F_{25}F_{34} - p_{25}p_{34}F_{23}F_{45} - GE_1$	$p_{24}p_{35}F_{25}F_{34} - p_{25}p_{34}F_{24}F_{35} - GE_1$	
<i>Group 2</i>	$F_{13}F_{45} - F_{14}F_{35} + F_{15}F_{34}$	$p_{13}p_{45}F_{14}F_{35} - p_{14}p_{35}F_{13}F_{45} - GE_2$	
	$p_{13}p_{45}F_{15}F_{34} - p_{15}p_{34}F_{13}F_{45} - GE_2$	$p_{14}p_{35}F_{15}F_{34} - p_{15}p_{34}F_{14}F_{35} - GE_2$	
<i>Group 3</i>	$F_{12}F_{45} - F_{14}F_{25} + F_{15}F_{24}$	$p_{12}p_{45}F_{14}F_{25} - p_{14}p_{25}F_{12}F_{45} - GE_3,$	
	$p_{12}p_{45}F_{15}F_{24} - p_{15}p_{24}F_{12}F_{45} - GE_3$	$p_{14}p_{25}F_{15}F_{24} - p_{15}p_{24}F_{14}F_{25} - GE_3$	
<i>Group 4</i>	$F_{12}F_{35} - F_{13}F_{25} + F_{15}F_{23}$	$p_{12}p_{35}F_{13}F_{25} - p_{13}p_{25}F_{12}F_{35} - GE_4$	
	$p_{12}p_{35}F_{15}F_{23} - p_{15}p_{23}F_{12}F_{35} - GE_4$	$p_{13}p_{25}F_{15}F_{23} - p_{15}p_{23}F_{13}F_{25} - GE_4$	
<i>Group 5</i>	$F_{12}F_{34} - F_{13}F_{24} + F_{14}F_{23}$	$p_{12}p_{34}F_{13}F_{24} - p_{13}p_{24}F_{12}F_{34} - GE_5$	
	$p_{12}p_{34}F_{14}F_{23} - p_{14}p_{23}F_{12}F_{34} - GE_5$	$p_{13}p_{24}F_{14}F_{23} - p_{14}p_{23}F_{13}F_{24} - GE_5$	
<i>Group 1'</i>	$p_{25}F_{12}E_2 - p_{35}F_{13}E_3 + p_{45}F_{14}E_4$	$p_{24}F_{12}E_2 - p_{34}F_{13}E_3 + p_{45}F_{15}E_5$	
	$p_{23}F_{12}E_2 - p_{34}F_{14}E_4 + p_{35}F_{15}E_5$	$p_{23}F_{13}E_3 - p_{24}F_{14}E_4 + p_{25}F_{15}E_5$	
<i>Group 2'</i>	$p_{15}F_{12}E_1 - p_{35}F_{23}E_3 + p_{45}F_{24}E_4$	$p_{14}F_{12}E_1 - p_{34}F_{23}E_3 + p_{45}F_{25}E_5$	
	$p_{13}F_{12}E_1 - p_{34}F_{24}E_4 + p_{35}F_{25}E_5$	$p_{13}F_{23}E_3 - p_{14}F_{24}E_4 + p_{15}F_{25}E_5$	
<i>Group 3'</i>	$p_{15}F_{13}E_1 - p_{25}F_{23}E_2 + p_{45}F_{34}E_4$	$p_{14}F_{13}E_1 - p_{24}F_{23}E_2 + p_{45}F_{35}E_5$	
	$p_{12}F_{13}E_1 - p_{24}F_{34}E_4 + p_{25}F_{35}E_5$	$p_{12}F_{23}E_2 - p_{14}F_{34}E_4 + p_{15}F_{35}E_5$	
<i>Group 4'</i>	$p_{15}F_{14}E_1 - p_{25}F_{24}E_2 + p_{35}F_{34}E_3$	$p_{13}F_{14}E_1 - p_{23}F_{24}E_2 + p_{35}F_{45}E_5$	
	$p_{12}F_{14}E_1 - p_{23}F_{34}E_3 + p_{25}F_{45}E_5$	$p_{12}F_{24}E_2 - p_{13}F_{34}E_3 + p_{15}F_{45}E_5$	
<i>Group 5'</i>	$p_{14}F_{15}E_1 - p_{24}F_{25}E_2 + p_{34}F_{35}E_3$	$p_{13}F_{15}E_1 - p_{23}F_{25}E_2 + p_{34}F_{45}E_4$	
	$p_{12}F_{15}E_1 - p_{23}F_{35}E_3 + p_{24}F_{45}E_4$	$p_{12}F_{25}E_2 - p_{13}F_{35}E_3 + p_{14}F_{45}E_4$	

Proposition 2.1 will be derived later in this section. For now, let us discuss the structure and symmetry of the generators of $I_{\mathcal{Y}}$. We consider the 5-dimensional *demicube*, here denoted D_5 . This is the convex hull of the following 16 points in the hyperplane $\{a_0 = 0\} \subset \mathbb{R}^6$:

$$\{(1, a_1, a_2, a_3, a_4, a_5) \in \{0, 1\}^6 : a_1 + a_2 + a_3 + a_4 + a_5 \text{ is odd}\}. \quad (2.4)$$

The group of symmetries of D_5 is the Weyl group $W(D_5)$. It acts transitively on (2.4). There is a natural bijection between the 16 variables in the Cox ring and the vertices of D_5 :

$$\begin{aligned} E_1 &\leftrightarrow (1, 1, 0, 0, 0, 0), E_2 \leftrightarrow (1, 0, 1, 0, 0, 0), \dots, E_5 \leftrightarrow (1, 0, 0, 0, 0, 1), \\ F_{12} &\leftrightarrow (1, 0, 0, 1, 1, 1), F_{13} \leftrightarrow (1, 0, 1, 0, 1, 1), \dots, F_{45} \leftrightarrow (1, 1, 1, 1, 0, 0), \\ G &\leftrightarrow (1, 1, 1, 1, 1, 1). \end{aligned} \quad (2.5)$$

This bijection defines the grading via the Picard group \mathbb{Z}^6 . We regard the p_{ij} as scalars, so they have degree 0. Generators of I_Y that are listed in the same group have the same \mathbb{Z}^6 degrees. The action of $W(D_5)$ on the demicube D_5 gives the action on the 16 variables.

Consider now a particular smooth del Pezzo surface X of degree 4 over the field K , so the p_{ij} are scalars in K that satisfy the Plücker relations in the Base Group. The universal Cox ideal I_Y specializes to the Cox ideal I_X for the particular surface X . That Cox ideal is minimally generated by 20 quadrics, two per group. The surface X^0 is the zero set of the ideal I_X inside $(\bar{K}^*)^{16}/(\bar{K}^*)^6$. The torus action is obtained from (2.5), in analogy to (2.2).

Proof of Proposition 1.2. We computed $\text{trop}(X^0)$ by applying `gfan` [13] to the ideal I_X . If $K = \mathbb{Q}$ with the trivial valuation then the output is the cone over the *Clebsch graph* in Fig. 1. This 5-regular graph records which pairs of (-1) -curves intersect on X . This also works over a field K with non-trivial valuation. The software `gfan` uses $K = \mathbb{Q}(t)$. If the vector (p_{12}, \dots, p_{45}) tropicalizes into the interior of an edge in the Petersen graph then $\text{trop}(X^0)$ is the tropical surface described in Proposition 1.2. Each node in Fig. 1 is replaced by a trivalent tree on 5 nodes according to the color coding explained in Section 1. The surface $\text{trop}(X^0)$ can also be determined by tropical modifications, as in Section 4. \square

The same tropicalization method works for the universal family \mathcal{Y}^0 . Its ideal I_Y is given by the 45 polynomials in 26 variables listed above, and \mathcal{Y}^0 is the zero set of I_Y in the 15-dimensional torus $(\bar{K}^*)^{10}/(\bar{K}^*)^5 \times (\bar{K}^*)^{16}/(\bar{K}^*)^6$. The tropical universal del Pezzo surface $\text{trop}(\mathcal{Y}^0)$ is a 4-dimensional fan in $\mathbb{R}^{26}/\mathbb{R}^{11}$. We compute it by applying `gfan` to the *universal Cox ideal* I_Y . The Gröbner fan structure on $\text{trop}(I_Y)$ has f-vector (76, 630, 1620, 1215). It is isomorphic to the *Naruki fan* described in [20, Table 5] and discussed further in Section 3.

Del Pezzo surfaces of degree 3 (Cubic surfaces)

There exists a cuspidal cubic through any six points in \mathbb{P}^2 . See e.g. [19, (4.4)] and [20, (6.1)]. Hence any configuration of six points in \mathbb{P}^2 can be represented by the columns of a matrix

$$D = \begin{pmatrix} 1 & 1 & 1 & 1 & 1 & 1 \\ d_1 & d_2 & d_3 & d_4 & d_5 & d_6 \\ d_1^3 & d_2^3 & d_3^3 & d_4^3 & d_5^3 & d_6^3 \end{pmatrix}.$$

The maximal minors of the matrix D factor into linear forms,

$$[ijk] = (d_i - d_j)(d_i - d_k)(d_j - d_k)(d_i + d_j + d_k), \quad (2.6)$$

and so does the condition for the six points to lie on a conic:

$$\begin{aligned} [\text{conic}] &= [134][156][235][246] - [135][146][234][256] \\ &= (d_1 + d_2 + d_3 + d_4 + d_5 + d_6) \cdot \prod_{1 \leq i < j \leq 6} (d_i - d_j). \end{aligned} \quad (2.7)$$

The linear factors in these expressions form the root system of type E_6 . This corresponds to an arrangement of 36 hyperplanes in \mathbb{P}^5 . Similarly, the arrangement of type E_7 consists of 63 hyperplanes in \mathbb{P}^6 , as in [19, (4.4)]. To be precise, for $m = 6, 7$, the roots for E_m are

$$\begin{aligned} d_i - d_j & \quad \text{for} \quad 1 \leq i < j \leq m, \\ d_i + d_j + d_k & \quad \text{for} \quad 1 \leq i < j < k \leq m, \\ d_{i_1} + d_{i_2} + \cdots + d_{i_6} & \quad \text{for} \quad 1 \leq i_1 < i_2 < \cdots < i_6 \leq m. \end{aligned} \quad (2.8)$$

Linear dependencies among these linear forms specify a matroid of rank m , also denoted E_m .

The moduli space of marked cubic surfaces is the 4-dimensional *Yoshida variety* \mathcal{Y} defined in [20, §6]. It coincides with the subvariety \mathcal{Y}^0 of $(\bar{K}^*)^{26}/(\bar{K}^*)^{11}$ cut out by the 45 trinomials in Proposition 2.1. This is the embedding of \mathcal{Y}^0 in its intrinsic torus, as in [20, Theorem 6.1], and it differs from the embedding of \mathcal{Y}^0 into $(\bar{K}^*)^{40}/(\bar{K}^*)$ referred to in Section 3 below.

The universal family for cubic surfaces is denoted by \mathcal{G}^0 . This is the open part of the *Göpel variety* $\mathcal{G} \subset \mathbb{P}^{134}$ constructed in [19, §5]. The base of this 6-dimensional family is the 4-dimensional \mathcal{Y}^0 . The map $\mathcal{G}^0 \rightarrow \mathcal{Y}^0$ was described in [11]. Thus the ring $K[\mathcal{Y}]$ in (2.3) is the natural base ring for the universal Cox ring for degree 3 surfaces.

At this point it is essential to avoid confusing notation. To aim for a clear presentation, we use the uniformization of \mathcal{Y} by the E_6 hyperplane arrangement. Namely, we take $R = \mathbb{Z}[d_1, d_2, d_3, d_4, d_5, d_6]$ instead of $K[\mathcal{Y}]$ as the base ring. We write \mathcal{X} for the universal cubic surface over R . The *universal Cox ring* is a quotient of the polynomial ring over R in 27 variables, one for each line on the cubic surface. Using variable names as in [26, §5], we write

$$\text{Cox}(\mathcal{X}) = R[E_1, E_2, \dots, E_6, F_{12}, F_{13}, \dots, F_{56}, G_1, G_2, \dots, G_6]/I_{\mathcal{X}}. \quad (2.9)$$

This ring is graded by the Picard group \mathbb{Z}^7 , similarly to (2.5). The role of the 5-dimensional demicube D_5 is now played by the 6-dimensional *Gosset polytope* with

27 vertices, here also denoted by E_6 . The symmetry group of this polytope is the Weyl group $W(E_6)$.

Proposition 2.2. *Up to saturation by the product of all 27 variables and all 36 roots, the universal Cox ideal $I_{\mathcal{X}}$ is generated by 270 trinomials. These are clustered by \mathbb{Z}^7 -degrees into 27 groups of 10 generators, one for each line on the cubic surface. For instance, the 10 generators of $I_{\mathcal{X}}$ that correspond to the line G_1 involve the 10 lines that meet G_1 . They are*

$$\begin{aligned} & (d_3-d_4)(d_1+d_3+d_4)E_2F_{12} - (d_2-d_4)(d_1+d_2+d_4)E_3F_{13} + (d_2-d_3)(d_1+d_2+d_3)E_4F_{14}, \\ & (d_3-d_5)(d_1+d_3+d_5)E_2F_{12} - (d_2-d_5)(d_1+d_2+d_5)E_3F_{13} + (d_2-d_3)(d_1+d_2+d_3)E_5F_{15}, \\ & (d_3-d_6)(d_1+d_3+d_6)E_2F_{12} - (d_2-d_6)(d_1+d_2+d_6)E_3F_{13} + (d_2-d_3)(d_1+d_2+d_3)E_6F_{16}, \\ & (d_4-d_5)(d_1+d_4+d_5)E_2F_{12} - (d_2-d_5)(d_1+d_2+d_5)E_4F_{14} + (d_2-d_4)(d_1+d_2+d_4)E_5F_{15}, \\ & (d_4-d_6)(d_1+d_4+d_6)E_2F_{12} - (d_2-d_6)(d_1+d_2+d_6)E_4F_{14} + (d_2-d_4)(d_1+d_2+d_4)E_6F_{16}, \\ & (d_5-d_6)(d_1+d_5+d_6)E_2F_{12} - (d_2-d_6)(d_1+d_2+d_6)E_5F_{15} + (d_2-d_5)(d_1+d_2+d_5)E_6F_{16}, \\ & (d_4-d_5)(d_1+d_4+d_5)E_3F_{13} - (d_3-d_5)(d_1+d_3+d_5)E_4F_{14} + (d_3-d_4)(d_1+d_3+d_4)E_5F_{15}, \\ & (d_4-d_6)(d_1+d_4+d_6)E_3F_{13} - (d_3-d_6)(d_1+d_3+d_6)E_4F_{14} + (d_3-d_4)(d_1+d_3+d_4)E_6F_{16}, \\ & (d_5-d_6)(d_1+d_5+d_6)E_3F_{13} - (d_3-d_6)(d_1+d_3+d_6)E_5F_{15} + (d_3-d_5)(d_1+d_3+d_5)E_6F_{16}, \\ & (d_5-d_6)(d_1+d_5+d_6)E_4F_{14} - (d_4-d_6)(d_1+d_4+d_6)E_5F_{15} + (d_4-d_5)(d_1+d_4+d_5)E_6F_{16}. \end{aligned}$$

The remaining 260 trinomials are obtained by applying the action of $W(E_6)$. The variety defined by $I_{\mathcal{X}}$ in $\mathbb{P}^5 \times (\bar{K}^*)^{27}/(\bar{K}^*)^7$ is 6-dimensional. It is the universal family \mathcal{X}^0 .

Proof of Propositions 2.1 and 2.2. We consider the prime ideal in [19, §6] that defines the embedding of the Göpel variety \mathcal{G} into \mathbb{P}^{134} . By [19, Theorem 6.2], \mathcal{G} is the ideal-theoretic intersection of a 35-dimensional toric variety \mathcal{T} and a 14-dimensional linear space L . The latter is cut out by a canonical set of 315 linear trinomials, indexed by the 315 isotropic planes in $(\mathbb{F}_2)^6$. Pulling these linear forms back to the Cox ring of \mathcal{T} , we obtain 315 quartic trinomials in 63 variables, one for each root of E_7 . Of these 63 roots, precisely 27 involve the unknown d_7 . We identify these with the (-1) -curves on the cubic surface via

$$d_i - d_7 \mapsto E_i, \quad d_i + d_j + d_7 \mapsto F_{ij}, \quad -d_j + \sum_{i=1}^7 d_i \mapsto G_j. \quad (2.10)$$

Moreover, of the 315 quartics, precisely 270 contain a root involving d_7 . Their images under the map (2.10) are the 270 Cox relations listed above. Our construction ensures that they generate the correct Laurent polynomial ideal on the torus of \mathcal{T} . This proves Proposition 2.2.

The derivation of Proposition 2.1 is similar, but now we use the substitution

$$d_i - d_6 \mapsto E_i, \quad d_i + d_j + d_6 \mapsto F_{ij}, \quad \sum_{i=1}^6 d_i \mapsto G.$$

We consider the 45 quartic trinomials that do not involve d_7 . Of these, precisely five do not involve d_6 either. They translate into the five Plücker relations for $M_{0,5}$. With this identification, the remaining 40 quartics translate into the ten groups listed after [Proposition 2.1](#). \square

Remark 2.3. The relations [\(2.10\)](#) is not unique. The non-uniqueness comes from both the symmetry of E_7 and the choice of \pm sign for each variable E_i, F_{ij}, G_j . For the rest of this paper, we fix the relations [\(2.10\)](#). Other choices give the same result up to symmetry.

We now fix a K -valued point in the base \mathcal{Y}^0 , by replacing the unknowns d_i with scalars in K . In order for the resulting surface X to be smooth, we require $(d_1 : d_2 : d_3 : d_4 : d_5 : d_6)$ to be in the complement of the 36 hyperplanes for E_6 . The corresponding specialization of $I_{\mathcal{X}}$ is the Cox ideal I_X of X . Seven of the ten trinomials in each degree are redundant over K . Only three are needed to generate I_X . Hence, the Cox ideal I_X is minimally generated by 81 quadrics in the E_i, F_{ij} and G_i . Its variety is the surface $X^0 = V(I_X) \subset (\bar{K}^*)^{27}/(\bar{K}^*)^7$.

Proposition 2.4. *Each of the marked 27 trees on a tropical cubic surface has an involution.*

Proof. Every line L on a cubic surface X over K , with its ten marked points, admits a double cover to \mathbb{P}^1 with five markings. The preimage of one of these marked points is the pair of markings on L given by two other lines forming a tritangent with L . Tropically, this gives a double cover from the 10-leaf tree for L to a 5-leaf tree with leaf labelings given by these pairs. The desired involution on the 10-leaf tree exchanges elements in each pair. \square

For instance, for the tree that corresponds to the line $L = G_1$, the involution equals

$$E_2 \leftrightarrow F_{12}, \quad E_3 \leftrightarrow F_{13}, \quad E_4 \leftrightarrow F_{14}, \quad E_5 \leftrightarrow F_{15}, \quad E_6 \leftrightarrow F_{16}.$$

Indeed, this involution fixes the 10 Cox relations displayed in [Proposition 2.2](#). The induced action on the trees corresponding to the tropicalization of the lines can be seen in [Figs. 4 and 5](#), where the involution reflects about a vertical axis. The corresponding 5-leaf tree is the tropicalization of the line in

$$\text{Proj}(K[E_2F_{12}, E_3F_{13}, E_4F_{14}, E_5F_{15}, E_6F_{16}]) \simeq \mathbb{P}^4$$

that is the intersection of the 10 hyperplanes defined by the polynomials in [Proposition 2.2](#).

We aim to compute $\text{trop}(X^0)$ by applying **gfan** to the ideal I_X . This works well for $K = \mathbb{Q}$ with the trivial valuation. Here the output is the cone over the *Schläfli graph* which records which pairs of (-1) -curves intersect on X . This is a 10-regular graph with 27 nodes. However, for $K = \mathbb{Q}(t)$, our **gfan** calculations did not terminate. Future

implementations of tropical algorithms will surely succeed, see also [Conjecture 5.3](#). To get the tropical cubic surfaces, and to prove [Theorem 1.1](#), we used the alternative method explained in [Section 3](#).

3. Sekiguchi fan to Naruki fan

In the previous section we discussed the computation of tropical del Pezzo surfaces directly from their Cox ideals. This worked well for degree 4. However, using the current implementation in `gfan`, this computation did not terminate for degree 3. We here discuss an alternative method that did succeed. In particular, we present the proof of [Theorem 1.1](#).

The successful computation uses the following commutative diagram of balanced fans:

$$\begin{array}{ccc} \text{Berg}(E_7) & \longrightarrow & \text{trop}(\mathcal{G}^0) \\ \downarrow & & \downarrow \\ \text{Berg}(E_6) & \longrightarrow & \text{trop}(\mathcal{Y}^0) \end{array} \quad (3.1)$$

This diagram was first derived by Hacking et al. [\[11\]](#), in their study of moduli spaces of marked del Pezzo surfaces. Combinatorial details were worked out by Ren et al. in [\[20, §6\]](#). The material that follows completes the program that was suggested at the very end of [\[20\]](#).

The notation $\text{Berg}(E_m)$ denotes the *Bergman fan* of the rank m matroid defined by the (36 resp. 63) linear forms listed in [\(2.8\)](#). Thus, $\text{Berg}(E_6)$ is a tropical linear space in \mathbb{TP}^{35} , and $\text{Berg}(E_7)$ is a tropical linear space in \mathbb{TP}^{62} . Coordinates are labeled by roots.

The list [\(2.8\)](#) fixes a choice of injection of root systems $E_6 \hookrightarrow E_7$. This defines coordinate projections $\mathbb{R}^{63} \rightarrow \mathbb{R}^{36}$ and $\mathbb{TP}^{62} \dashrightarrow \mathbb{TP}^{35}$, namely by deleting coordinates with index 7. This projection induces the vertical map from $\text{Berg}(E_7)$ to $\text{Berg}(E_6)$ on the left in [\(3.1\)](#).

On the right in [\(3.1\)](#), we see the 4-dimensional *Yoshida variety* $\mathcal{Y} \subset \mathbb{P}^{39}$ and the 6-dimensional *Göpel variety* $\mathcal{G} \subset \mathbb{P}^{134}$. Explicit parametrizations and equations for these varieties were presented in [\[19, 20\]](#). The corresponding very affine varieties $\mathcal{G}^0 \subset (\bar{K}^*)^{135}/\bar{K}^*$ and $\mathcal{Y}^0 \subset (\bar{K}^*)^{40}/\bar{K}^*$ are moduli spaces of marked del Pezzo surfaces [\[11\]](#). Their tropicalizations $\text{trop}(\mathcal{G}^0)$ and $\text{trop}(\mathcal{Y}^0)$ are known as the *Sekiguchi fan* and *Naruki fan*, respectively. The modular interpretation in [\[11\]](#) ensures the existence of the vertical map $\text{trop}(\mathcal{G}^0) \rightarrow \text{trop}(\mathcal{Y}^0)$. This map is described in [\[11, Lemma 5.4\]](#), in [\[20, \(6.5\)\]](#), and in the proof of [Lemma 3.1](#) below.

The two horizontal maps in [\(3.1\)](#) are surjective and (classically) linear. The linear map $\text{Berg}(E_7) \rightarrow \text{trop}(\mathcal{G}^0)$ is given by the 135×63 matrix A in [\[19, §6\]](#). The corresponding toric variety is the object of [\[19, Theorem 6.1\]](#). The map $\text{Berg}(E_6) \rightarrow \text{trop}(\mathcal{Y}^0)$ is given by the 40×36 -matrix in [\[20, Theorem 6.1\]](#). We record the following computational result. It refers to the natural simplicial fan structure on $\text{Berg}(E_m)$ described by Ardila et al. in [\[3\]](#).

Lemma 3.1. *The Bergman fans of E_6 and E_7 have dimensions 5 and 6. Their f -vectors are*

$$\begin{aligned} f_{\text{Berg}(E_6)} &= (1, 750, 17679, 105930, 219240, 142560), \\ f_{\text{Berg}(E_7)} &= (1, 6091, 315399, 3639804, 14982660, 24607800, 13721400). \end{aligned}$$

The moduli fans $\text{trop}(\mathcal{Y}^0)$ and $\text{trop}(\mathcal{G}^0)$ have dimensions 4 and 6. Their f -vectors are

$$\begin{aligned} f_{\text{trop}(\mathcal{Y}^0)} &= (1, 76, 630, 1620, 1215), \\ f_{\text{trop}(\mathcal{G}^0)} &= (1, 1065, 27867, 229243, 767025, 1093365, 547155). \end{aligned}$$

Proof. The f -vector for the Naruki fan $\text{trop}(\mathcal{Y}^0)$ appears in [20, Table 5]. For the other three fans, only the numbers of rays (namely 750, 6091 and 1065) were known from [20, §6]. The main new result in Lemma 3.1 is the computation of all 57273155 cones in $\text{Berg}(E_7)$. The fans $\text{Berg}(E_6)$ and $\text{trop}(\mathcal{G}^0)$ are subsequently derived from $\text{Berg}(E_7)$ using the maps in (3.1).

We now describe how $f_{\text{Berg}(E_7)}$ was found. We did not use the theory of tubings in [3]. Instead, we carried out a brute force computation based on [10] and [21]. Recall that a point lies in the Bergman fan of a matroid if and only if the minimum is obtained twice on each circuit. We computed all circuits of the rank 7 matroid on the 63 vectors in the root system E_7 . That matroid has precisely 100662348 circuits. Their cardinalities range from 3 to 8. This furnishes a subroutine for deciding whether a given point lies in the Bergman fan.

Our computations were mostly done in `sage` [24] and `java`. We achieved speed by exploiting the action of the Weyl group $W(E_7)$ given by the two generators in [19, (4.2)]. The two matrices derived from these two generators using [19, (4.3)] act on the space \mathbb{R}^7 with coordinates d_1, d_2, \dots, d_7 . This gives subroutines for the action of $W(E_7)$ on \mathbb{R}^{63} , e.g. for deciding whether two given sequences of points are conjugate with respect to this action.

Let $\mathbf{r}_1, \dots, \mathbf{r}_{6091}$ denote the rays of $\text{Berg}(E_7)$, as in [11, Table 2] and [20, §6]. They form 11 orbits under the action of $W(E_7)$. For each orbit, we take the representative \mathbf{r}_i with smallest label. For each pair $i < j$ such that \mathbf{r}_i is a representative, our program checks if $\mathbf{r}_i + \mathbf{r}_j$ lies in $\text{Berg}(E_7)$, using the precomputed list of circuits. If yes, then \mathbf{r}_i and \mathbf{r}_j span a 2-dimensional cone in $\text{Berg}(E_7)$. This process gives representatives for the $W(E_7)$ -orbits of 2-dimensional cones. The list of all cones is produced by applying the action of $W(E_7)$ on the result. For each orbit, we keep only the lexicographically smallest representative $(\mathbf{r}_i, \mathbf{r}_j)$.

Next, for each triple $i < j < k$ such that $(\mathbf{r}_i, \mathbf{r}_j)$ is a representative, we check if $\mathbf{r}_i + \mathbf{r}_j + \mathbf{r}_k$ lies in $\text{Berg}(E_7)$. If so, then $\{\mathbf{r}_i, \mathbf{r}_j, \mathbf{r}_k\}$ spans a 3-dimensional cone in $\text{Berg}(E_7)$. The list of all 3-dimensional cones can be found by applying the action of $W(E_7)$ on the result. As before, we fix the lexicographically smallest representatives. Repeating this process for dimensions 4, 5 and 6, we obtain the list of all cones in $\text{Berg}(E_7)$ and hence the f -vector of this fan.

We now describe the procedure to derive $\text{trop}(\mathcal{G}^0)$ by applying the top horizontal map $\phi : \text{Berg}(E_7) \rightarrow \text{trop}(\mathcal{G}^0)$. Each ray \mathbf{r} in $\text{Berg}(E_7)$ maps to either (a) $\mathbf{0}$, (b) a ray of $\text{trop}(\mathcal{G}^0)$, or (c) a positive linear combination of 2 or 3 rays, as listed in [20, §6]. For each ray in case (c), our program iterates through all pairs and triples of rays in $\text{trop}(\mathcal{G}^0)$ and writes the image explicitly as a positive linear combination of rays. With this data, we give a first guess of $\text{trop}(\mathcal{G}^0)$ as follows: for each maximal cone $\sigma = \text{span}(\mathbf{r}_{i_1}, \dots, \mathbf{r}_{i_6})$ of $\text{Berg}(E_7)$, we write $\phi(\mathbf{r}_{i_1}), \dots, \phi(\mathbf{r}_{i_6})$ as linear combinations of the rays of $\text{trop}(\mathcal{G}^0)$ and take $\sigma' \subset \mathbb{TP}^{134}$ to be the cone spanned by all rays of $\text{trop}(\mathcal{G}^0)$ that appear in the linear combinations. From this we get a list of 6-dimensional cones σ' . Let $\Phi \subset \mathbb{TP}^{134}$ be the union of these cones.

To certify that $\Phi = \text{trop}(\mathcal{G}^0)$ we need to show (1) for each $\sigma \in \text{Berg}(E_7)$, we have $\phi(\sigma) \subset \sigma'$ for some cone $\sigma' \subset \Phi$; (2) each cone $\sigma' \subset \Phi$ is the union of some $\phi(\sigma)$ for $\sigma \in \text{Berg}(E_7)$; and (3) the intersection of any two cones σ'_1, σ'_2 in Φ is a face of both σ'_1 and σ'_2 . The claim (1) follows from the procedure of constructing Φ . For (2), one only needs to verify the cases where σ' is one of the 9 representatives by the action of $W(E_7)$. For each of these, our program produces a list of $\phi(\sigma)$, and we check manually that σ' is indeed the union. For (3), one only needs to iterate through the cases where σ'_1 is a representative, and the procedure is straightforward. Therefore, our procedure shows that Φ is exactly $\text{trop}(\mathcal{G}^0)$. Then the f -vector is obtained from the list of all cones in the fan Φ .

Finally, we recover the list of all cones in $\text{Berg}(E_6)$ and $\text{trop}(\mathcal{Y}^0)$ by following the same procedure with the left vertical map and the bottom horizontal map. \square

Remark 3.2. The (reduced) Euler characteristic of the link of $\text{Berg}(E_7)$ is the alternating sum of the entries of the f -vector of this Bergman fan. We see from Lemma 3.1 that this is

$$\begin{aligned} 1 - 6091 + 315399 - 3639804 + 14982660 - 24607800 + 13721400 \\ = 765765 = 1 \cdot 5 \cdot 7 \cdot 9 \cdot 11 \cdot 13 \cdot 17. \end{aligned}$$

This is the product of all exponents of $W(E_7)$, thus confirming the prediction in [19, (9.2)].

The Naruki fan $\text{trop}(\mathcal{Y}^0)$ is studied in [20, §6]. Under the action of $W(E_6)$ through $\text{Berg}(E_6)$, it has two classes of rays, labeled type (a) and type (b). It also has two $W(E_6)$ -orbits of maximal cones: there are 135 type (aaaa) cones, each spanned by four type (a) rays, and 1080 type (aaab) cones, each spanned by three type (a) rays and one type (b) ray.

The map $\text{trop}(\mathcal{G}^0) \rightarrow \text{trop}(\mathcal{Y}^0)$ tropicalizes the morphism $\mathcal{G}^0 \rightarrow \mathcal{Y}^0$ between very affine K -varieties of dimension 6 and 4. That morphism is the universal family of cubic surfaces. In order to tropicalize these surfaces, we examine the fibers of the map $\text{trop}(\mathcal{G}^0) \rightarrow \text{trop}(\mathcal{Y}^0)$. The next lemma concerns the subdivision of $\text{trop}(\mathcal{Y}^0)$ induced by this map. By definition, this is the coarsest subdivision such that each cone in $\text{trop}(\mathcal{G}^0)$ is sent to a union of cones.

Lemma 3.3. *The subdivision induced by the map $\text{trop}(\mathcal{G}^0) \rightarrow \text{trop}(\mathcal{Y}^0)$ is the barycentric subdivision on type (aaaa) cones. For type (aaab) cones, each cone in the subdivision is a cone spanned by the type (b) ray and a cone in the barycentric subdivision of the (aaa) face. Thus each (aaaa) cone is divided into 24 cones, and each (aaab) cone is divided into 6 cones.*

Proof. The map $\pi : \text{trop}(\mathcal{G}^0) \rightarrow \text{trop}(\mathcal{Y}^0)$ can be defined via the commutative diagram (3.1): for $\mathbf{x} \in \text{trop}(\mathcal{G}^0)$, take any point in its preimage in $\text{Berg}(E_7)$, then follow the left vertical map and the bottom horizontal map to get $\pi(\mathbf{x})$ in $\text{trop}(\mathcal{Y}^0)$. It is well-defined because the kernel of the map $\text{Berg}(E_7) \rightarrow \text{trop}(\mathcal{G}^0)$ is contained in the kernel of the composition $\text{Berg}(E_7) \rightarrow \text{Berg}(E_6) \rightarrow \text{trop}(\mathcal{Y}^0)$. With this, we can compute the image in $\text{trop}(\mathcal{Y}^0)$ of any cone in $\text{trop}(\mathcal{G}^0)$. For each orbit of cones in $\text{trop}(\mathcal{Y}^0)$, pick a representative σ , and examine all cones in $\text{trop}(\mathcal{G}^0)$ that map into σ . Their images reveal the subdivision of σ . \square

Lemma 3.3 shows that each (aaaa) cone of the Naruki fan $\text{trop}(\mathcal{Y}^0)$ is divided into 24 subcones, and each (aaab) cone is divided into 6 subcones. Thus, the total number of cones in the subdivision is $24 \times 135 + 6 \times 1080 = 9720$. For the base points in the interior of a cone, the fibers are contained in the same set of cones in $\text{trop}(\mathcal{G}^0)$. The fiber changes continuously as the base point changes. Therefore, moving the base point around the interior of a cone simply changes the metric but not the combinatorial type of marked tropical cubic surface.

Corollary 3.4. *The map $\text{trop}(\mathcal{G}^0) \rightarrow \text{trop}(\mathcal{Y}^0)$ has at most two combinatorial types of generic fibers up to relabeling.*

Proof. We fixed an inclusion $E_6 \hookrightarrow E_7$ in (2.8). The action of $\text{Stab}_{E_6}(W(E_7))$ on the fans is compatible with the entire commutative diagram (3.1). Hence, the fibers over two points that are conjugate under this action have the same combinatorial type. We verify that the 9720 cones form exactly two orbits under this action. One orbit consists of the cones in the type (aaaa) cones, and the other consists of the cones in the type (aaab) cones. Therefore, there are at most two combinatorial types, one for each orbit. \square

We can now derive our classification theorem for tropical cubic surfaces.

Proof of Theorem 1.1. We compute the two types of fibers of $\pi : \text{trop}(\mathcal{G}^0) \rightarrow \text{trop}(\mathcal{Y}^0)$. In what follows we explain this for a cone σ of type (aaaa). The computation for type (aaab) is similar. Let $\mathbf{r}_1, \mathbf{r}_2, \mathbf{r}_3, \mathbf{r}_4$ denote the rays that generate σ . We fix the vector $\mathbf{x} = \mathbf{r}_1 + 2\mathbf{r}_2 + 3\mathbf{r}_3 + 4\mathbf{r}_4$ that lies in the interior of a cone in the barycentric subdivision.

The fiber $\pi^{-1}(\mathbf{x})$ is found by an explicit computation. First we determine the directions of the rays. They arise from rays of $\text{trop}(\mathcal{G}^0)$ that are mapped to zero by π . There are 27 such ray directions in $\pi^{-1}(\mathbf{x})$. These are exactly the image of the 27 type A_1 rays in $\text{Berg}(E_7)$ that correspond to the roots in $E_7 \setminus E_6$. We label them by E_i, F_{ij}, G_j as

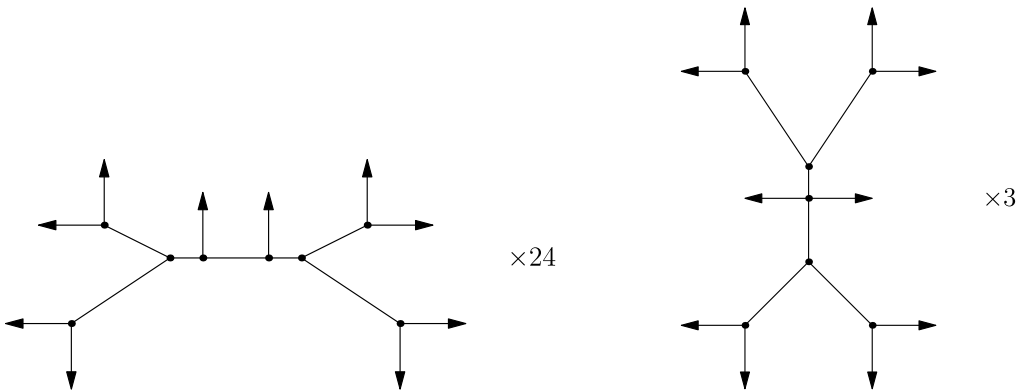


Fig. 4. The 27 trees on tropical cubic surfaces of type (aaaa).

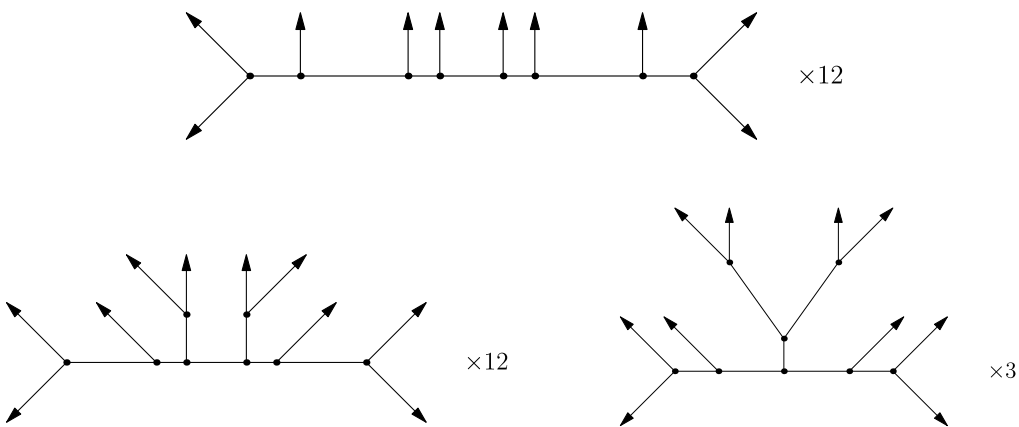


Fig. 5. The 27 trees on tropical cubic surfaces of type (aaab).

in (2.10). Next, we compute the vertices of $\pi^{-1}(\mathbf{x})$. They are contained in 4-dimensional cones $\sigma' = \text{pos}\{\mathbf{R}_1, \mathbf{R}_2, \mathbf{R}_3, \mathbf{R}_4\}$ with $\mathbf{x} \in \pi(\sigma')$. The coordinates of each vertex in \mathbb{TP}^{134} is computed by solving $y_1\pi(\mathbf{R}_1) + y_2\pi(\mathbf{R}_2) + y_3\pi(\mathbf{R}_3) + y_4\pi(\mathbf{R}_4) = \mathbf{x}$ for y_1, y_2, y_3, y_4 .

The part of the fiber contained in each cone in $\text{trop}(\mathcal{G}^0)$ is spanned by the vertices and the E_i, F_{ij}, G_j rays it contains. Iterating through the list of cones and looking at this data, we get a list that characterizes the polyhedral complex $\pi^{-1}(\mathbf{x})$. In particular, that list verifies that $\pi^{-1}(\mathbf{x})$ is 2-dimensional and has the promised f-vector. For each of the 27 ray directions E_i, F_{ij}, G_j , there is a tree at infinity. It is the link of the corresponding point at infinity $\pi^{-1}(\mathbf{x}) \subset \mathbb{TP}^{134}$. The combinatorial types of these 27 trees are shown in Fig. 4. The metric on each tree can be computed as follows: the length of a bounded edge equals the lattice distance between the two vertices in the corresponding flap.

The surface $\pi^{-1}(\mathbf{x})$ is homotopy equivalent to its bounded complex. We check directly that the bounded complex is contractible. This can also be inferred from Theorem 4.4. \square

Remark 3.5. We may replace $\mathbf{x} = \mathbf{r}_1 + 2\mathbf{r}_2 + 3\mathbf{r}_3 + 4\mathbf{r}_4$ with a generic point $\mathbf{x} = x_1\mathbf{r}_1 + x_2\mathbf{r}_2 + x_3\mathbf{r}_3 + x_4\mathbf{r}_4$, where $x_1 < x_2 < x_3 < x_4$. This lies in the same cone in the barycentric subdivision, so the combinatorics of $\pi^{-1}(\mathbf{x})$ remains the same. Repeating the last step over the field $\mathbb{Q}(x_1, x_2, x_3, x_4)$ instead of \mathbb{Q} , we write the length of each bounded edge in the 27 trees in terms of the parameters. Each length either equals x_1, x_2, x_3, x_4 or is $x_i - x_j$ for some i, j .

4. Tropical modifications

In Section 2 we computed tropical varieties from polynomial ideals, along the lines of the book by Maclagan and Sturmfels [15]. We now turn to tropical geometry as a self-contained subject in its own right. This is the approach presented in the book by Mikhalkin and Rau [17]. Central to that approach is the notion of tropical modification. In this section we explain how to construct our tropical del Pezzo surfaces from the plane \mathbb{R}^2 by modifications. This leads to proofs of Proposition 1.2 and Theorem 1.1 purely within tropical geometry.

Tropical modification is an operation that relates topologically different tropical models of the same variety. This operation was first defined by Mikhalkin in [16], see also [17, Chapter 5]. Here we work with a variant known as *open tropical modifications*. These were introduced in the context of Bergman fans of matroids in [23]. Brugallé and Lopez de Medrano [7] used them to study intersections and inflection points of tropical plane curves.

We fix a tropical cycle Y in \mathbb{R}^n , as in [17]. An *open modification* is a map $p : Y' \rightarrow Y$ where $Y' \subset \mathbb{R}^{n+1}$ is a new tropical variety to be described below. One should think of Y' as being an embedding of the complement of a divisor in Y into a higher-dimensional torus.

Consider a piecewise integer affine function $g : Y \rightarrow \mathbb{R}$. The graph

$$\Gamma_g(Y) = \{(y, g(y)) \mid y \in Y\} \subset \mathbb{R}^{n+1}$$

is a polyhedral complex which inherits weights from Y . However, it usually not balanced. There is a canonical way to turn $\Gamma_g(Y)$ into a balanced complex. If $\Gamma_g(Y)$ is unbalanced around a codimension one face E , then we attach to it a new unbounded facet F_E in direction $-e_{n+1}$. (We here use the max convention, as in [17].) The facet F_E can be equipped with a unique weight $w_{F_E} \in \mathbb{Z}$ such that the complex obtained by adding F_E is balanced at E . The resulting tropical cycle is $Y' \subset \mathbb{R}^{n+1}$. By definition, the *open modification* of Y given by g is the map $p : Y' \rightarrow Y$, where p comes from the projection $\mathbb{R}^{n+1} \rightarrow \mathbb{R}^n$ with kernel $\mathbb{R}e_{n+1}$.

The *tropical divisor* $\text{div}_Y(g)$ consists of all points $y \in Y$ such that $p^{-1}(y)$ is infinite. This is a polyhedral complex. It inherits weights on its top-dimensional faces from those of Y' . A tropical cycle is *effective* if the weights of its top-dimensional faces are positive. Therefore, the cycle Y' is effective if and only if Y and the divisor $\text{div}_Y(g)$ are effective.

Given a tropical variety Y and an effective divisor $\text{div}_Y(g)$, we say the *tropical modification* $p : Y' \rightarrow Y$ is *along* $\text{div}_Y(g)$. See [16,17,23] for basics concerning cycles, divisors and modifications.

Open tropical modifications are related to re-embeddings of classical varieties as follows. Fix a very affine K -variety $X \subset (\bar{K}^*)^n$ and $Y = \text{trop}(X) \subset \mathbb{R}^n$. Given a polynomial function $f \in K[X]$, let D be its divisor in X . Then $X \setminus D$ is isomorphic to the graph of the restriction of f to $X \setminus D$. In this manner, the function f gives a closed embedding of $X \setminus D$ into $(\bar{K}^*)^{n+1}$.

For the next proposition we require the tropicalization of a variety to be *locally irreducible*. Let y be a point in a tropical variety Y . We note that

$$\text{Star}_y(Y) = \{y' \mid \exists \epsilon > 0 \text{ s.t. } \forall 0 < \delta < \epsilon : y + \epsilon y' \in Y\}$$

is a balanced tropical fan with weights inherited from Y . A tropical variety Y is *locally irreducible* if at every point $y \in Y$, we have that $\text{Star}_y(Y)$ is not a proper union of two tropical varieties, taking weights into consideration.

Proposition 4.1. *Let $X \subset (\bar{K}^*)^n$ be a very affine variety. For a function $f \in K[X]$, let D be the divisor $\text{div}_X(f)$, and let $X' = X \setminus D \subset (\bar{K}^*)^{n+1}$ denote the graph of X along f as described above. Let $Y = \text{trop}(X) \subset \mathbb{R}^n$ and $Y' = \text{trop}(X') \subset \mathbb{R}^{n+1}$. Suppose that Y is locally irreducible. Then there exists a piecewise integer affine function $g : Y \rightarrow \mathbb{R}$ such that $\text{div}_Y(g) = \text{trop}(D)$ and the coordinate projection $Y' \rightarrow Y$ is the open modification of Y along that divisor.*

Proof. The coordinate projection $p : \mathbb{R}^{n+1} \rightarrow \mathbb{R}^n$ takes Y' onto Y , since tropicalization acts coordinate-wise. We claim that the fiber over a point $y \in Y$ is either a single point or a half-line in the $-e_{n+1}$ direction. The fiber $p^{-1}(y)$ is 1-dimensional and closed in Y' . Let y' be an endpoint of a connected component of $p^{-1}(y)$. Then $p(\text{Star}_{y'}(Y'))$ has the same dimension as Y . Since otherwise, $\text{Star}_{y'}(Y')$ contains a space of linearity in the direction e_{n+1} and y' cannot be an endpoint of the fiber. If the one dimensional fiber $p^{-1}(y)$ contains two endpoints y_1 and y_2 then Y must be reducible at y ; it can be split into more than one component coming from the projection of $p(\text{Star}_{y_1}(Y'))$ and $p(\text{Star}_{y_2}(Y'))$. Therefore, $p^{-1}(y)$ consists of either a single point, a line, or a half line. However, since $f \in K[X]$ is a regular function, the fiber of a point $y \in Y$ cannot be unbounded in the $+e_{n+1}$ direction. Thus the only possibilities are that $p^{-1}(y)$ is a single point or a half line in the $-e_{n+1}$ direction.

Finally, we obtain the piecewise integer affine function g by taking $g(y) = p^{-1}(y)$ for $y \in Y \setminus \text{trop}(D)$ and then extending by continuity to the rest of Y . Then Y' is the modification along the function g described above. \square

Any two tropical rational functions g and g' that define the same tropical divisor on Y must differ by a map which is integer affine on Y , see [1, Remark 3.6]. This leads to the following corollary.

Corollary 4.2. *Under the assumptions of Proposition 4.1, the tropicalization of $X' = X \setminus D \subset \mathbb{R}^{n+1}$ is determined uniquely by those of D and X , up to an integer affine map.*

In general, $\text{trop}(X')$ is not determined by the tropical hypersurface of $f \in K[X]$, as the tropicalization of the divisor $D = \text{div}_X(f)$ may differ from the tropical stable intersection of $\text{trop}(X')$ and that tropical hypersurface. Examples 4.2 and 4.3 of [7] demonstrate both this and that Proposition 4.1 can fail without the locally irreducibility hypothesis.

Suppose now that $X' \subset (\bar{K}^*)^{n+k}$ is obtained from $X \subset (\bar{K}^*)^n$ by taking the graph of a list of $k \geq 2$ polynomials f_1, f_2, \dots, f_k . This gives us a sequence of projections

$$X' = X_k \rightarrow X_{k-1} \rightarrow \cdots \rightarrow X_2 \rightarrow X_1 \rightarrow X_0 = X, \quad (4.1)$$

where $X_i \subset (\bar{K}^*)^{n+i}$ is obtained from X by taking the graph of (f_1, \dots, f_i) . We further get a corresponding sequence of projections of the tropicalizations:

$$\text{trop}(X') = \text{trop}(X_k) \rightarrow \text{trop}(X_{k-1}) \rightarrow \cdots \rightarrow \text{trop}(X_0) = \text{trop}(X). \quad (4.2)$$

We may ask if it is possible to recover $\text{trop}(X') \subset \mathbb{R}^{n+k}$ just from $\text{trop}(X)$ and the k tropical divisors $\text{trop}(D_i)$ considered in $\text{trop}(X)$. The answer is “yes” in the special case when $\text{trop}(X) = \mathbb{R}^n$ and the arrangement of divisors $\text{trop}(D_i)$ are each locally irreducible and intersect properly, meaning the intersection of any l of these divisors has codimension l . However, in general, iterating modifications to recover $\text{trop}(X')$ is a delicate procedure. In most cases, the outcome is not solely determined by the configuration of tropical divisors in $\text{trop}(X)$, even if the divisors intersect pairwise properly. We illustrate this by deriving the degree 5 del Pezzo surface $\text{trop}(M_{0,5})$.

Example 4.3. This is a variation on [23, Example 2.29]. Let $X = (\bar{K}^*)^2$ and consider the functions $f(x) = x_1 - 1$, $g(x) = x_2 - 1$ and $h(x) = ax_1 - x_2$, for some constant $a \in K^*$ with $\text{val}(a) = 0$. Denote $\text{div}_X(f)$ by F , and analogously for G and H . The tropicalization of each divisor is a line through the origin in \mathbb{R}^2 . The directions of $\text{trop}(F)$, $\text{trop}(G)$, and $\text{trop}(H)$ are $(1, 0)$, $(0, 1)$, and $(1, 1)$ respectively. Let $X' \subset (\bar{K}^*)^5$ denote the graph of X along the three functions f , g , and h , in that order. This defines a sequence of projections,

$$X' \longrightarrow X_2 \longrightarrow X_1 \longrightarrow X = (\bar{K}^*)^2.$$

Here, $X_2 = \{(x_1, x_2, x_1 - 1, x_2 - 1)\} \subset (\bar{K}^*)^4$. The tropical plane $\text{trop}(X_2)$ contains the face $\sigma = \{0\} \times \{0\} \times (-\infty, 0] \times (-\infty, 0]$, corresponding to points with $\text{val}(x_1) = \text{val}(x_2) = 0$. Let H_2 denote the graph of f and g restricted to H . This is a line in 4-space, namely,

$$H_2 = \{(x_1, ax_1, x_1 - 1, ax_1 - 1)\} \subset X_2 \subset (\bar{K}^*)^4.$$

The tropical line $\text{trop}(H_2)$ depends on the valuation of $a - 1$. It can be determined from

$$\text{trop}(G_1 \cap H_1) = \left\{ \left(0, 0, -\text{val}\left(\frac{1}{a} - 1\right) \right) \right\}.$$

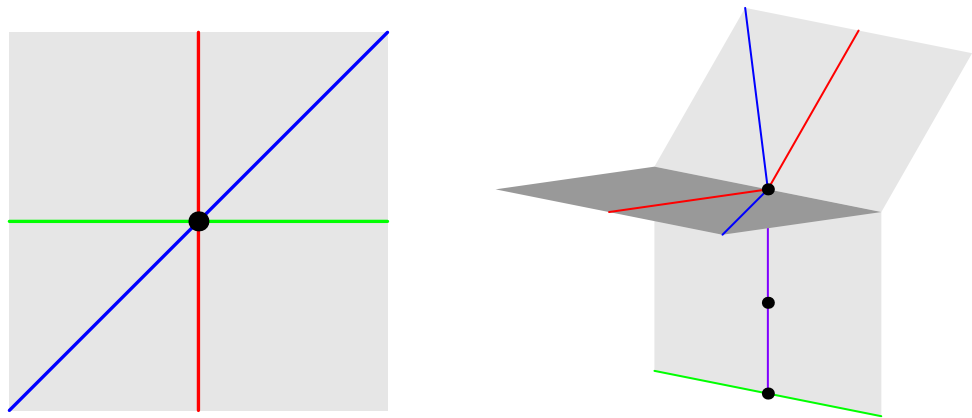


Fig. 6. The tropical divisors in Example 4.3. The positions of $\text{trop}(G_1 \cap H_1)$ in $\text{trop}(X_1)$ for three choices of a are marked on the downward purple edge. For $a = 1$ we get $M_{0,5}$. (For interpretation of the references to color in this figure legend, the reader is referred to the web version of this article.)

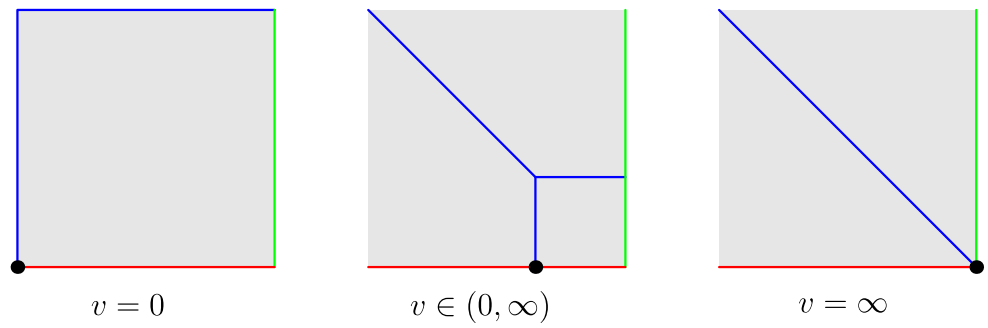


Fig. 7. The different possibilities for $\text{trop}(H_2) \cap \sigma$ in Example 4.3.

Here, H_1, G_1 denote the graph of f restricted to H and G , respectively. Fig. 6 shows the possibilities for $\text{trop}(G_1 \cap H_1)$ in $\text{trop}(X_1)$, and Fig. 7 shows $\text{trop}(H_2) \cap \sigma$ in $\text{trop}(X_2)$.

We can prescribe any value $v \in (0, \infty)$ for the valuation of $\frac{1}{a} - 1$, for instance by taking $\frac{1}{a} = 1 + t^v$ when $K = \mathbb{C}\{\{t\}\}$. In these cases, the tropical plane $\text{trop}(X')$ is not a fan. However, it becomes a fan when v moves to either endpoint of the interval $[0, -\infty]$. For instance, $v = 0$ happens when the constant term of $\frac{1}{a}$ is not equal to 1 and $\text{trop}(X')$ is the fan obtained from \mathbb{R}^2 by carrying out the modifications along the pull-backs of the tropical divisors on the left in Fig. 6. See Definition 2.16 of [23] for pull-backs of tropical divisors. The other extreme is when $a = 1$. Here, F, G, H are concurrent lines in $(\bar{K}^*)^2$, and $\text{trop}(H_2)$ contains a ray in the direction $e_3 + e_4$. Upon modification, we obtain the fan over the Petersen graph in Fig. 3. This is the tropicalization of the degree 5 del Pezzo surface in (2.2). Thus beginning from the tropical divisors $\text{trop}(F), \text{trop}(G)$, and $\text{trop}(H)$ in \mathbb{R}^2 , we recover $\text{trop}(M_{0,5})$ if we know that they represent tropicalizations of concurrent lines in $(\bar{K}^*)^2$.

The open tropical modification described above represents the tropicalization of the very affine variety $M_{0,5}$. The compactification of $M_{0,5}$ which produces the del Pezzo surface of degree 5 is the tropical compactification given by the fan $\text{trop}(M_{0,5})$, (see [15, §6.4] for an introduction to tropical compactifications). There is no direct connection between open tropical modifications and birational transformations. Relationship depends a choice of compactification of the very affine variety. Upon removing divisors one can find more interesting compactifications of the complement. For example, $(K^*)^2$ cannot be compactified to a del Pezzo surface of degree less than 6, but upon deleting the three divisors above one can compactify the complement to a del Pezzo surface of degree 5. \diamond

We now explain how this extends to a del Pezzo surface X of degree $d \leq 4$. As before, we write X^0 for the complement of the (-1) -curves in X . Then $X' = X^0$ is obtained from $(\bar{K}^*)^2$ by taking the graphs of the polynomials f_1, \dots, f_k of the curves in $(\bar{K}^*)^2$ that give rise to (-1) -curves on X . More precisely, fix $p_1 = (1 : 0 : 0)$, $p_2 = (0 : 1 : 0)$, $p_3 = (0 : 0 : 1)$, $p_4 = (1 : 1 : 1)$, and take p_5, \dots, p_{9-d} to be general points in \mathbb{P}^2 . If $d = 4$ then there is only one extra point p_5 , we have $k = 8$ in (4.1), and f_1, \dots, f_8 are the polynomials defining

$$F_{14}, F_{15}, F_{24}, F_{25}, F_{34}, F_{35}, F_{45}, G. \quad (4.3)$$

For $d = 3$, there are two extra points p_5, p_6 in X , we have $k = 18$, and f_1, \dots, f_{18} represent

$$F_{14}, F_{15}, F_{16}, F_{24}, F_{25}, F_{26}, F_{34}, F_{35}, F_{36}, F_{45}, F_{46}, F_{56}, G_1, G_2, G_3, G_4, G_5, G_6. \quad (4.4)$$

We write $P_i = \text{trop}(p_i) \in \mathbb{TP}^2$ for the image of the point p_i under tropicalization. The tropical points P_1, P_2, \dots are in *general position* if any two lie in a unique tropical line, these lines are distinct, any five lie in a unique tropical conic, and these conics are distinct in \mathbb{TP}^2 . A configuration in general position for $d = 4$ is shown in Fig. 8. Our next result implies that the colored Clebsch graph in Fig. 1 can be read off from Fig. 8 alone. For $d = 3$, in order to recover the tropical cubic surface from the planar configuration, the points P_i must satisfy further genericity assumptions, to be revealed in the proof of the next theorem.

Theorem 4.4. Fix $d \in \{3, 4, 5\}$ and points p_1, \dots, p_{9-d} in \mathbb{P}^2 whose tropicalizations P_i are sufficiently generic in \mathbb{TP}^2 . The tropical del Pezzo surface $\text{trop}(X^0)$ can be constructed from \mathbb{TP}^2 by a sequence of open modifications that is determined by the points P_1, \dots, P_{9-d} .

Proof. The sequence of tropical modifications we use to go from \mathbb{R}^2 to $\text{trop}(X^0)$ is determined if we know, for each i , the correct divisor on each (-1) -curve C in the tropical

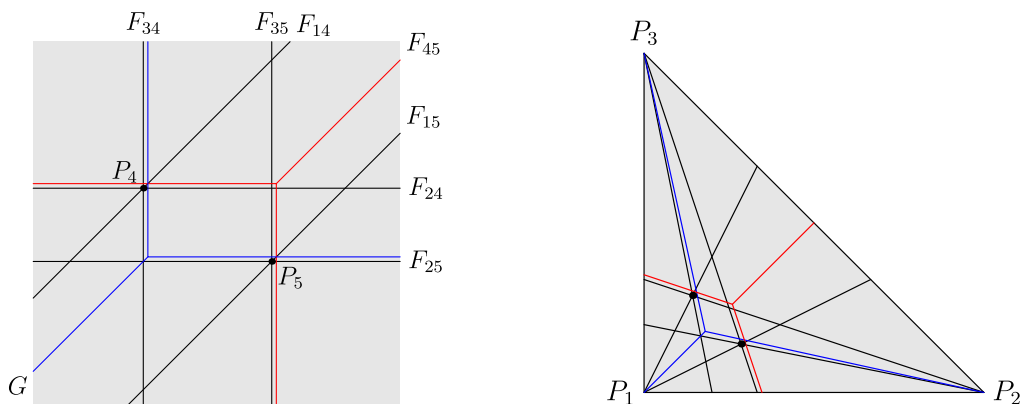


Fig. 8. The tropical conic and the tropical lines determined by the 5 points for a marked del Pezzo surface of degree 4. The diagram is drawn in \mathbb{R}^2 on the left and in \mathbb{TP}^2 on the right. The 16 trivalent trees corresponding to the (-1) -curves of the del Pezzo surface, seen at the nodes in Fig. 1, arise from the plane curves shown here by tropical modifications. (For interpretation of the references to color in this figure, the reader is referred to the web version of this article.)

model $\text{trop}(X_i)$. Then, the preimage of C in the next surface $\text{trop}(X_{i+1})$ is the modification C' of the curve C along that divisor. By induction, each intermediate surface $\text{trop}(X_i)$ is locally irreducible, since it is obtained by modifying a locally irreducible surface along a locally irreducible divisor. With this, Theorem 4.4 follows from Proposition 4.1, applied to both the i -th surface and its (-1) -curves. The case $d = 5$ was covered in Example 4.3. From the metric tree that represents the boundary divisor C of X^0 we can derive the corresponding trees on each intermediate surface $\text{trop}(X_i)$ by deleting leaves. Thus, to establish Theorem 4.4, it suffices to prove the following claim: *the final arrangement of the (16 or 27) metric trees on the tropical del Pezzo surface $\text{trop}(X^0)$ is determined by the locations of the points P_i in \mathbb{TP}^2 .*

Consider first the case $d = 4$. The points P_4 and P_5 determine an arrangement of plane tropical curves (4.3) as shown in Fig. 8. The conic G through all five points looks like an “inverted tropical line”, with three rays in directions P_1, P_2, P_3 . By the genericity assumption, the points P_4 and P_5 are located on distinct rays of G . These data determine a trivalent metric tree with five leaves, which we now label by E_1, E_2, E_3, E_4, E_5 . Namely, P_4 forms a cherry together with the label of its ray, and ditto for P_5 . For instance, in Fig. 8, the cherries on the tree G are $\{E_1, E_4\}$ and $\{E_2, E_5\}$, while E_3 is the non-cherry leaf. This is precisely the tree sitting on the node labeled G in Fig. 1. The lengths of the two bounded edges of the tree G are the distances from P_4 resp. P_5 to the unique vertex of the conic G in \mathbb{R}^2 . Thus the metric tree G is easily determined from P_4 and P_5 . The other 15 metric trees can also be determined in a similar way from the configuration of points and curves in \mathbb{R}^2 and by performing a subset of the necessary modifications. Alternatively, we may use the transition rules (1.1) and (1.2) to obtain the other 15 trees from G . This proves the above claim, and hence Theorem 4.4, for del Pezzo surfaces of degree $d = 4$.

Consider now the case $d = 3$. Here the arrangement of tropical plane curves in $\mathbb{R}^2 \subset \mathbb{TP}^2$ consists of three lines at infinity, F_{12}, F_{13}, F_{23} , nine straight lines, $F_{14}, F_{15}, \dots, F_{36}$, three honest tropical lines, F_{45}, F_{46}, F_{56} , three conics that are “inverted tropical lines” G_4, G_5, G_6 , and three conics with one bounded edge, G_1, G_2, G_3 . Each of these looks like a tree already in the plane, and it gets modified to a 10-leaf tree, like to ones in Figs. 4 and 5. We claim that these labeled metric trees are uniquely determined by the positions of P_4, P_5, P_6 in \mathbb{R}^2 .

Consider one of the 9 straight lines in our arrangement, say, F_{14} . If the points P_4, P_5, P_6 are generically chosen, 7 of the 10 leaves on the tree F_{ij} can be determined from the diagram in \mathbb{R}^2 . These come from the 7 markings on the line F_{14} given by $E_1, E_4, F_{23}, F_{25}, F_{26}, F_{35}, F_{36}$. The markings E_1 and F_{23} are the points at infinity, the marking E_4 is the location of point P_4 , and the markings $F_{25}, F_{26}, F_{35}, F_{36}$ are the points of intersection with those lines. Under our hypothesis, these 7 marked points on the line F_{14} will be distinct. With this, F_{14} is already a metric caterpillar tree with 7 leaves. The three markings which are missing are G_1, G_4 and F_{56} . Depending on the positions of P_4, P_5, P_6 , the intersection points of these three curves with the line F_{14} may coincide with previously marked points. Whenever this happens, the position of the additional marking on the tree F_{14} can be anywhere on the already attached leaf ray. Again, the actual position of the point on that ray may be determined by performing modifications along those curves. Alternatively, we use the involution given in Corollary 2.4. The involution on the ten leaves of the desired tree F_{14} is

$$E_1 \leftrightarrow \underline{G_4}, \quad E_4 \leftrightarrow \underline{G_1}, \quad F_{23} \leftrightarrow \underline{F_{56}}, \quad F_{25} \leftrightarrow F_{36}, \quad F_{26} \leftrightarrow F_{35}.$$

Since the involution exchanges each of the three unknown leaves with one of the seven known leaves, we can easily construct the final 10-leaf tree from the 7-leaf caterpillar.

A similar argument works the other six lines F_{ij} , and the conics G_4, G_5, G_6 . In these cases, 8 of the 10 marked points on a tree are determined from the arrangement in the plane, provided the choice of points is generic. Finally, the conics G_1, G_2, G_3 are dual to subdivisions of lattice parallelograms of area 1. They may contain a bounded edge. Suppose no point P_j lies on the bounded edge of the conic G_i , then the positions of all 10 marked points of the tree are visible from the arrangement in the plane. If G_i does contain a marked point P_j on its bounded edge, then the tropical line F_{ij} intersects G_i in either a bounded edge or a single point with intersection multiplicity 2, depending on the dual subdivision of G_i . In the first case the position of the marked point F_{ij} is easily determined from the involution; the distance from a vertex of the bounded edge of G_i to the marked point F_{ij} must be equal to the distance from P_j to the opposite vertex of the bounded edge of G_i .

If $G_i \cap F_{ij}$ is a single point of intersection multiplicity two, then P_j and F_{ij} form a cherry on the tree G_i which is invariant under the involution. We claim that this cherry attaches to the rest of the tree at a 4-valent vertex. The involution on the 10-leaf tree can also be seen as a tropical double cover from our 10-leaf tree to a 5-leaf tree,

$h : T \rightarrow t$, where the 5-leaf tree t is labeled with the pair of markings interchanged by the involution. As mentioned in [Corollary 2.4](#), this double cover comes from the classical curve in the del Pezzo surface X . In particular, the double cover locally satisfies the tropical translation of the Riemann–Hurwitz condition [[5](#), [Definition 2.2](#)]. In our simple case of a degree 2 map between two trees, this local condition for a vertex v of T is $\deg(v) - d_{h,v}(\deg(h(v)) - 2) - 2 \geq 0$, where \deg denotes the valency of a vertex, and $d_{h,v}$ denotes the local degree of the map h at v . Suppose the two leaves did not attach at a four valent vertex, then they form a cherry, this cherry attaches to the rest of the tree by an edge e which is adjacent to another vertex v of the tree. The Riemann–Hurwitz condition is violated at v , since $\deg(v) = \deg(h(v)) = 3$ and $d_{h,v} = 2$.

We conclude that the tree arrangement can be recovered from the position of the points P_1, P_2, \dots in \mathbb{R}^2 . Therefore it is also possible to recover the tropical del Pezzo surface $\text{trop}(X^0)$ by open modifications. In each case, we recover the corresponding final 10 leaf tree from the arrangement in \mathbb{TP}^2 plus our knowledge of the involution in [Corollary 2.4](#). \square

Remark 4.5. Like in the case $d = 4$, knowledge of transition rules among the 27 metric trees on $\text{trop}(X^0)$ can greatly simplify their reconstruction. We give such a rule in [Proposition 5.2](#).

In this section we gave a geometric construction of tropical del Pezzo surfaces of degree $d \geq 3$, starting from the points P_1, \dots, P_{9-d} in the tropical plane \mathbb{TP}^2 . The lines and conics in \mathbb{TP}^2 that correspond to the (-1) -curves are transformed, by a sequence of open tropical modifications, into the trees that make up the boundary of the del Pezzo surface. Knowing these well-specified modifications of curves ahead of time allows us to carry out a unique sequence of open tropical modifications of surfaces, starting with \mathbb{R}^2 . In each step, going from right to left in [\(4.1\)](#), we modify the surface along a divisor given by one of the trees.

This gives a geometric construction for the bounded complex in a tropical del Pezzo surface: it is the preimage under [\(4.1\)](#) of the bounded complex in the arrangement in \mathbb{R}^2 . For instance, [Fig. 2](#) is the preimage of the parallelogram and the four triangles in [Fig. 8](#).

The same modification approach can be used to construct (the bounded complexes of) any tropical plane in \mathbb{TP}^n from its tree arrangement. This provides a direct link between the papers [[12](#)] and [[23](#)]. That link should be useful for readers of the text books [[15](#)] and [[17](#)].

5. Tropical cubic surfaces and their 27 trees

This section is devoted to the combinatorial structure of tropical cubic surfaces. Throughout, X is a smooth del Pezzo surface of degree 3, without Eckhart points, and X^0 the very affine surface obtained by removing the 27 lines from X . Recall that an *Eckhart point* is an ordinary triple point in the union of the (-1) -curves. Going well

beyond the summary statistics of [Theorem 1.1](#), we now offer an in-depth study of the combinatorics of the surface $\text{trop}(X^0)$.

We begin with the construction of $\text{trop}(X^0)$ from six points in \mathbb{TP}^2 , as in [Section 4](#). The points P_5 and P_6 are general in $\mathbb{R}^2 \subset \mathbb{TP}^2$. The first four points are the coordinate points

$$P_1 = (0 : -\infty : -\infty), P_2 = (-\infty : 0 : -\infty), P_3 = (-\infty : -\infty : 0), P_4 = (0 : 0 : 0). \quad (5.1)$$

[Theorem 4.4](#) tells us that $\text{trop}(X^0)$ is determined by the locations of P_5 and P_6 when the points are generically chosen. There are two generic types, namely (aaaa) and (aaab), as shown in [Figs. 4 and 5](#). This raises the question of how the type can be decided from the positions of P_5 and P_6 . To answer that question, we shall use *tropical convexity* [[15, §5.2](#)]. There are five generic types of tropical triangles, depicted here in [Figs. 11 and 12](#). The unique 2-cell in such a tropical triangle has either 3, 4, 5 or 6 vertices. Two of these have 4 vertices, but only one type contains a parallelogram. That is the type which gives (aaaa).

Theorem 5.1. *Suppose that the tropical cubic surface constructed as in [Theorem 4.4](#) has one of the two generic types. Then it has type (aaaa) if and only if the 2-cell in the tropical triangle spanned by P_4 , P_5 and P_6 is a parallelogram. In all other cases, it has type (aaab).*

Note that the condition that the six points P_i are in general position is not sufficient to imply that the tropical cubic surface is generic. In some cases, the corresponding point in the Naruki fan $\text{trop}(\mathcal{Y}^0)$ will lie on the boundary of the subdivision induced by the map from $\text{trop}(\mathcal{G}^0)$, as described in [Section 3](#) and below. If so, the tropical cubic surface is degenerate.

Proof of [Theorem 5.1](#). The tree arrangements for the two types of generic surfaces consist of distinct combinatorial types, i.e. there is no overlap in [Figs. 4 and 5](#). Therefore, when the tropical cubic surface is generic, it is enough to determine the combinatorial type of a single tree. We do this for the conic G_1 . Given our choices of points [\(5.1\)](#) in \mathbb{TP}^2 , the tropical conic G_1 is dual to the Newton polygon with vertices $(0, 0)$, $(1, 0)$, $(0, 1)$, and $(1, 1)$. The triangulation has one interior edge, either of slope 1 or of slope -1 . We claim the following:

The tropical cubic surface $\text{trop}(X^0)$ has type (aaaa) if and only if the following holds:

1. *The bounded edge of the conic G_1 has slope -1 and contains a marked point P_j , or*
2. *the bounded edge of the conic G_1 has slope 1 and contains a marked point P_j , and the other two points P_j, P_k lie on opposite sides of the line spanned by the bounded edge.*

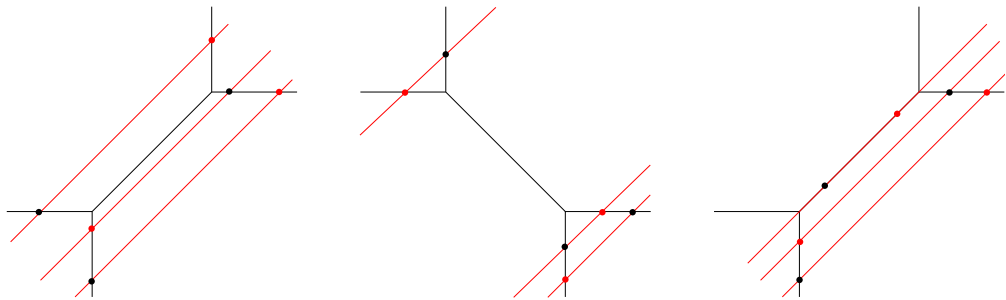


Fig. 9. Markings of a conic G_1 which produce trees of type (aaab).

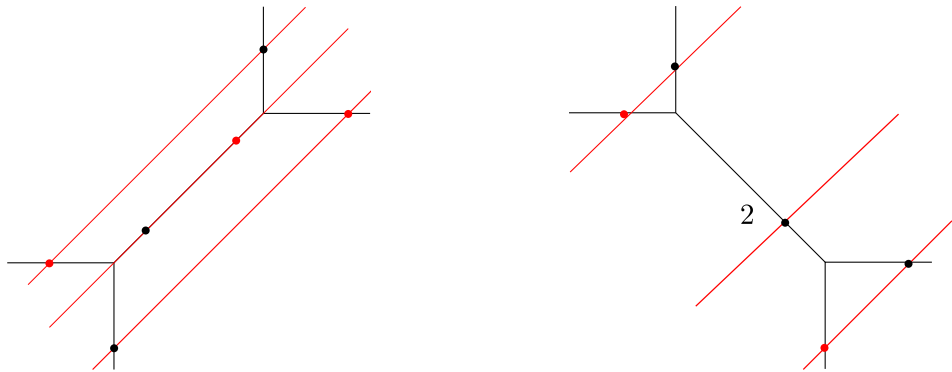


Fig. 10. Markings of a conic G_1 which produce trees of type (aaaa).

To show this, we follow the proof of [Theorem 4.4](#). For each configuration of P_4, P_5, P_6 on the conic G_1 , we draw lines with slope 1 through these points. These are the tropical lines F_{14}, F_{15}, F_{16} . Each intersects G_1 at one further point. These are the images of E_4, E_5, E_6 under the tree involution, i.e. the points labeled F_{14}, F_{15}, F_{16} on the tree G_1 . Together with E_2, E_3, F_{12} and F_{13} lying at infinity of \mathbb{TP}^2 , we can reconstruct a tree with 10 leaves. Then, we can identify the type of the tree arrangement. We did this for all possible configurations up to symmetry. Some of the results are shown in [Figs. 9 and 10](#). The claim follows.

To derive the theorem from the claim, we must consider the tropical convex hull of the points P_4, P_5, P_6 in the above cases. As an example, the 2-cells of the tropical triangle corresponding to the trees in [Figs. 9 and 10](#) are shown in [Figs. 11 and 12](#) respectively. The markings of G_1 producing a type (aaaa) tree always give parallelograms. Finally, if the marking of a conic produces a type (aaab) tree then the 2-cell may have 3, 4, 5, or 6 vertices. However, if it has 4 vertices, then it is a trapezoid with only one pair of parallel edges. \square

We next discuss some relations among the 27 boundary trees of a tropical cubic surface X . Any pair of disjoint (-1) -curves on X meets exactly five other (-1) -curves.

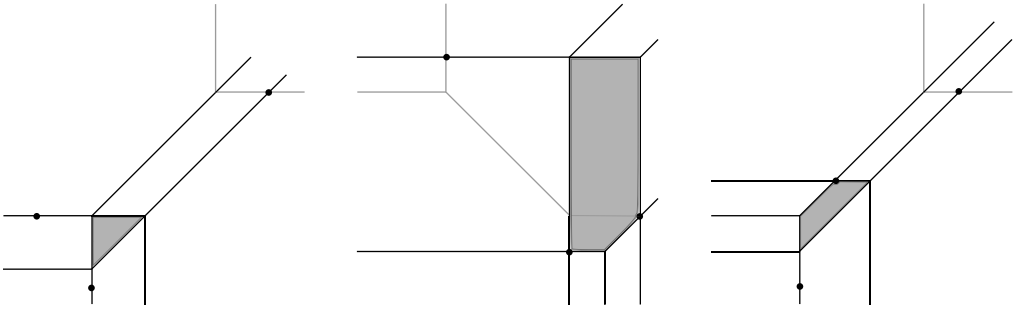


Fig. 11. The tropical triangles formed by points on G_1 as in Fig. 9, giving type (aaab).

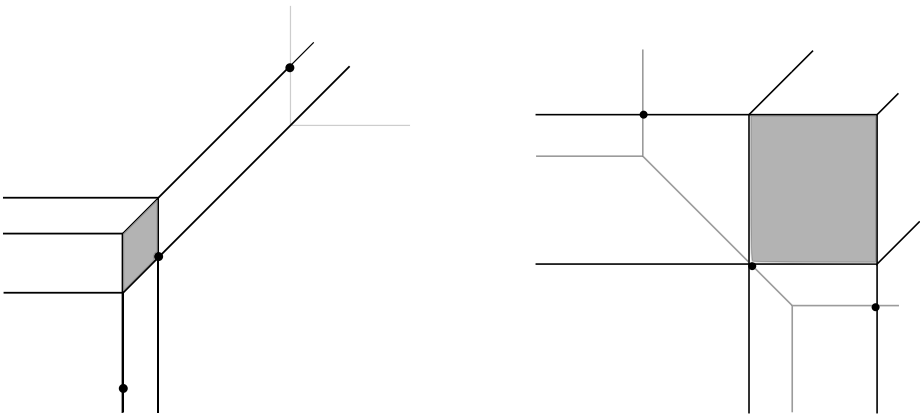


Fig. 12. The tropical triangles formed by points on G_1 as in Fig. 10, giving type (aaaa).

Thus, two 10-leaf trees T and T' representing disjoint (-1) -curves have exactly five leaf labels in common. Let t and t' denote the 5-leaf trees constructed from T and T' as in the proof of Proposition 2.4. Thus T double-covers t , and T' double-covers t' . Given a subset E of the leaf labels of a tree T , we write $T|_E$ for the subtree of T that is spanned by the leaves labeled with E .

Proposition 5.2. *Let T and T' be the trees corresponding to disjoint (-1) -curves on a cubic surface X , and E the set of five leaf labels common to T and T' . Then $t = T'|_E$ and $t' = T|_E$.*

Proof. The five lines that meet two disjoint (-1) -curves C and C' define five points on C and five tritangent planes containing C' . The cross-ratios among the former are equal to the cross-ratios among the latter modulo C' , see [18, Section 4]. The proposition follows because the metric trees can be derived from the valuations of all the various cross ratios. \square

Table 1
All combinatorial types of tropical cubic surfaces.

Type	#cones in moduli	Vertices	Edges	Rays	Triangles	Squares	Flaps	Cones
0	1	1	0	27	0	0	0	135
(a)	36	8	13	69	6	0	42	135
(a ₂)	270	20	37	108	14	4	81	135
(a ₃)	540	37	72	144	24	12	117	135
(a ₄)	1620	59	118	177	36	24	150	135
(b)	40	12	21	81	10	0	54	135
(aa ₂)	540	23	42	114	13	7	87	135
(aa ₃)	1620	43	82	156	22	18	129	135
(aa ₄)	540	68	133	195	33	33	168	135
(a ₂ a ₃)	1620	43	82	156	22	18	129	135
(a ₂ a ₄)	810	71	138	201	32	36	174	135
(a ₃ a ₄)	540	68	133	195	33	33	168	135
(ab)	360	26	48	123	16	7	96	135
(a ₂ b)	1080	45	86	162	24	18	135	135
(a ₃ b)	1080	69	135	198	34	33	171	135
(aa ₂ a ₃)	3240	46	87	162	21	21	135	135
(aa ₂ a ₄)	1620	74	143	207	31	39	180	135
(aa ₃ a ₄)	1620	74	143	207	31	39	180	135
(a ₂ a ₃ a ₄)	1620	74	143	207	31	39	180	135
(aa ₂ b)	2160	48	91	168	23	21	141	135
(aa ₃ b)	3240	75	145	210	32	39	183	135
(a ₂ a ₃ b)	3240	75	145	210	32	39	183	135
(aa ₂ a ₃ a ₄)	3240	77	148	213	30	42	186	135
(aa ₂ a ₃ b)	6480	78	150	216	31	42	189	135

[Proposition 5.2](#) suggests a combinatorial method for recovering the entire arrangement of 27 trees on $\text{trop}(X^0)$ from a single tree T . Namely, for any tree T' that is disjoint from T , we can recover both t' and $T'|_E$. Moreover, for any of the 10 trees T_i that are disjoint from both T and T' , with labels E_i common with T , we can determine $T'|_{E_i}$ as well. Then T' is an amalgamation of t' , $T'|_E$, and the 10 subtrees $T'|_{E_i}$. This amalgamation process is reminiscent of a tree building algorithm in phylogenetics known as *quartet puzzling* [\[9\]](#).

We next examine tropical cubic surfaces of non-generic types. These surfaces are obtained from non-generic fibers of the vertical map on the right in [\(3.1\)](#). We use the subdivision of the Naruki fan $\text{trop}(\mathcal{Y}^0)$ described in [Lemma 3.3](#). There are five types of rays in this subdivision. We label them (a), (b), (a₂), (a₃), (a₄). A ray of type (a_k) is a positive linear combination of k rays of type (a). The new rays (a₂), (a₃), (a₄) form the barycentric subdivision of an (aaaa) cone. With this, the maximal cones in the subdivided Naruki fan are called (aa₂a₃a₄) and (aa₂a₃b). They are known as the generic types (aaaa) and (aaab) in the previous sections. A list of all 24 cones, up to symmetry, is presented in the first column of [Table 1](#).

The fiber of $\text{trop}(\mathcal{G}^0) \rightarrow \text{trop}(\mathcal{Y}^0)$ over any point in the interior of a maximal cone is a tropical cubic surface. However, some special fibers have dimension 3. Such fibers

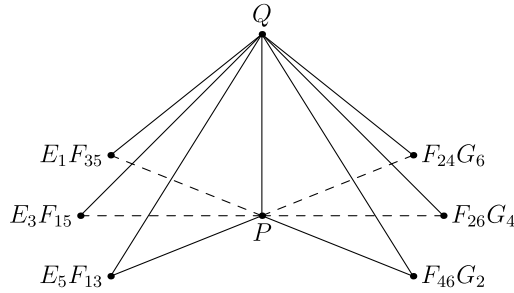


Fig. 13. The bounded complex of the tropical cubic surface of type (a).

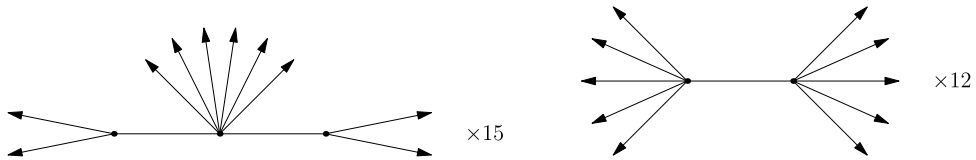


Fig. 14. The 27 trees on the tropical cubic surface of type (a).

contain infinitely many tropical cubic surfaces, including those with Eckhart points. Removing such Eckhart points is a key issue in [11]. We do this by considering the *stable fiber*, i.e. the limit of the generic fibers obtained by perturbing the base point by an infinitesimal. Alternatively, the tree arrangement of the stable fiber is found by setting some edge lengths to 0 in Remark 3.5. We computed representatives for all stable fibers. Our results are shown in Table 1.

We explain the two simplest non-trivial cases. The 36 type (a) rays in the Naruki fan are in bijection with the 36 positive roots of E_6 . Fig. 13 shows the bounded cells in the stable fiber over the (a) ray corresponding to root $r = d_1 + d_3 + d_5$. It consists of six triangles sharing a common edge. The two shared vertices are labeled by P and Q . Recall the identification of the roots of E_6 involving d_7 with the 27 (-1) -curves from (2.10). Then, considering E_i , F_{ij} and G_i as roots of E_6 , exactly 15 of them are orthogonal to r . The other 12 roots are

$$E_1, F_{35}; \quad E_3, F_{15}; \quad E_5, F_{13}; \quad F_{24}, G_6; \quad F_{26}, G_4; \quad F_{46}, G_2. \quad (5.2)$$

These form a *Schläfli double six*. The 36 double six configurations on a cubic surface are in bijection with the 36 positive roots of E_6 . Each of the six pairs forms an A_2 subroot system with $d_1 + d_3 + d_5$. The non-shared vertices in the (a) surface are labeled by these pairs.

The 12 rays labeled by (5.2) emanate from Q , and the other 15 rays emanate from P . Each other vertex has 7 outgoing rays, namely its labels in Fig. 13 and the 5 roots orthogonal to both of these. Fig. 14 shows the resulting $27 = 12 + 15$ trees at infinity.

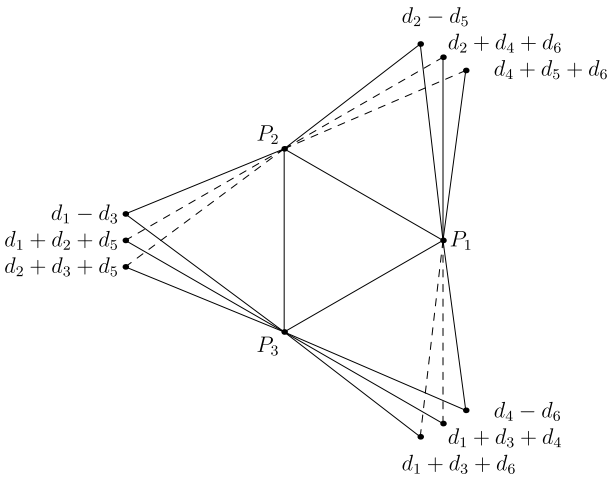


Fig. 15. The bounded complex of the tropical cubic surface of type (b).

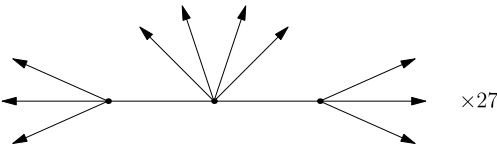


Fig. 16. The 27 trees on the tropical cubic surface of type (b).

The 40 type (b) rays in the Naruki fan are in bijection with the type $A_2^{\times 3}$ subroot systems in E_6 . Fig. 15 illustrates the stable fiber over a point lying on the ray corresponding to

$$\begin{aligned} & d_1 - d_3, \, d_1 + d_2 + d_5, \, d_2 + d_3 + d_5, \\ & d_2 - d_5, \, d_2 + d_4 + d_6, \, d_4 + d_5 + d_6, \\ & d_4 - d_6, \, d_1 + d_3 + d_4, \, d_1 + d_3 + d_6. \end{aligned} \tag{5.3}$$

This is the union of three type A_2 subroot systems that are pairwise orthogonal. The bounded complex consists of 10 triangles. The central triangle $P_1P_2P_3$ has 3 other triangles attached to each edge. The 9 pendant vertices are labeled with the roots in (5.3). The 3 vertices in the triangles attached to the same edge are labeled with 3 roots in a type A_2 subroot system.

Each of P_1 , P_2 and P_3 is connected with 9 rays, labeled with the roots in $E_7 \setminus E_6$ that are orthogonal to a type A_2 subroot system in (5.3). Each of the other vertices is connected with 6 rays. The labels of these rays are the roots in $E_7 \setminus E_6$ that are orthogonal to the label of that vertex but are not orthogonal to the other two vertices in the same group.

All of the 27 trees are isomorphic, as shown in Fig. 16. In each tree, the 10 leaves are partitioned into $10 = 4 + 3 + 3$, by orthogonality with the type A_2 subroot systems

in (5.3). The bounded part of the tree is connected by two flaps to two edges containing the same P_i .

We close this paper with a brief discussion of open questions and future directions. One obvious question is whether our construction can be extended to del Pezzo surfaces of degree $d = 2$ and $d = 1$. In principle, this should be possible, but the complexity of the algebraic and combinatorial computations will be very high. In particular, the analogues of Theorem 4.4 for 7 and 8 points in \mathbb{TP}^2 are likely to require rather complicated genericity hypotheses.

For $d = 4$, we were able to compute the Naruki fan $\text{trop}(\mathcal{Y}^0)$ without any prior knowledge, by just applying the software `gfan` to the 45 trinomials in Proposition 2.1. We believe that the same will work for $d = 3$, and that even the tropical basis property [15, §2.6] will hold:

Conjecture 5.3. *The 270 trinomial relations listed in Proposition 2.2 form a tropical basis.*

This paper did not consider embeddings of del Pezzo surfaces into projective spaces. However, it would be very interesting to study these via the results obtained here. For cubic surfaces in \mathbb{P}^3 , we should see a shadow of Table 1 in \mathbb{TP}^3 . Likewise, for complete intersections of two quadrics in \mathbb{P}^4 , we should see a shadow of Figs. 1 and 2 in \mathbb{TP}^4 . One approach is to start with the following tropical modifications of the ambient spaces \mathbb{TP}^3 resp. \mathbb{TP}^4 . Consider a graded component in (2.1) with \mathcal{L} very ample. Let $N + 1$ be the number of monomials in E_i, F_{ij}, G_k that lie in $H^0(X, \mathcal{L})$. The map given by these monomials embeds X into a linear subspace of \mathbb{P}^N . The corresponding tropical surfaces in \mathbb{TP}^N should be isomorphic to the tropical del Pezzo surfaces constructed here. In particular, if $\mathcal{L} = -K$ is the anticanonical bundle, then the subspace has dimension d , and the ambient dimensions are $N = 44$ for $d = 3$, and $N = 39$ for $d = 4$. In the former case, the 45 monomials (like $E_1 F_{12} G_2$ or $F_{12} F_{34} F_{56}$) correspond to Eckhart triangles. In the latter case, the 40 monomials (like $E_1 E_2 F_{12} G$ or $E_1 F_{12} F_{13} F_{45}$) are those of degree $(4, 2, 2, 2, 2, 2)$ in the grading (2.5). The tropicalizations of these *combinatorial anticanonical embeddings*, $X \subset \mathbb{P}^3 \subset \mathbb{P}^{44}$ for $d = 3$ and $X \subset \mathbb{P}^4 \subset \mathbb{P}^{39}$ for $d = 4$, should agree with our surfaces here. This will help in resolving remaining issues surrounding the excess of lines in tropical cubic surfaces. Examples of the superabundance of tropical lines on generic smooth tropical cubic hypersurfaces were first found by Vigeland [27] and these examples were later considered in [6] and [8].

One last consideration concerns cubic surfaces defined over \mathbb{R} . A cubic surface equipped with a real structure induces another involution on the 27 metric trees corresponding to real (-1) -curves. These trees already come partitioned by combinatorial type, depending on the type of tropical cubic surface. One could ask which trees can result from real lines, and whether the tree arrangement reveals Segre's partition of real lines on cubic surfaces into hyperbolic and elliptic types [22]. For example, for the (aaaa) and (aaab) types, if the involution on the trees from the real structure is the trivial one,

then the trees with combinatorial type occurring exactly three times always correspond to hyperbolic real lines.

Acknowledgments

This project started during the 2013 program on *Tropical Geometry and Topology* at the Max-Planck Institut für Mathematik in Bonn, with Kristin Shaw and Bernd Sturmfels in residence. Qingchun Ren and Bernd Sturmfels were supported by NSF grant DMS-0968882. Kristin Shaw had support from the Alexander von Humboldt Foundation in the form of a Postdoctoral Research Fellowship. We are grateful to Maria Angelica Cueto, Anand Deopurkar and also an anonymous referee for helping us to improve this paper.

References

- [1] L. Allermann, J. Rau, First steps in tropical intersection theory, *Math. Z.* 264 (3) (2010) 633–670.
- [2] F. Ardila, C. Klivans, The Bergman complex of a matroid and phylogenetic trees, *J. Combin. Theory Ser. B* 96 (1) (2006) 38–49.
- [3] F. Ardila, R. Reiner, L. Williams, Bergman complexes, Coxeter arrangements, and graph associahedra, *Sém. Lothar. Combin.* 54A (2006) B54Aj.
- [4] V. Batyrev, O. Popov, The Cox ring of a del Pezzo surface, in: *Arithmetic of Higher-Dimensional Algebraic Varieties*, in: *Progr. Math.*, vol. 226, Birkhäuser, Boston, 2004, pp. 85–103.
- [5] B. Bertrand, E. Brugallé, G. Mikhalkin, Tropical open Hurwitz numbers, *Rend. Semin. Mat. Univ. Padova* 125 (2011) 157–171.
- [6] T. Bogart, E. Katz, Obstructions to lifting tropical curves in surfaces in 3-space, *SIAM J. Discrete Math.* 26 (3) (2012) 1050–1067.
- [7] E. Brugallé, L. Lopez de Medrano, Inflection points of real and tropical plane curves, *J. Singul.* 3 (2012) 74–103.
- [8] E. Brugallé, K. Shaw, Obstructions to approximating tropical curves in surfaces via intersection theory, *Canad. J. Math.* 67 (3) (2015) 527–572.
- [9] D. Bryant, M. Steel, Constructing optimal trees from quartets, *J. Algorithms* 38 (2001) 237–259.
- [10] E. Feichtner, B. Sturmfels, Matroid polytopes, nested sets and Bergman fans, *Port. Math.* 62 (2005) 437–468.
- [11] P. Hacking, S. Keel, J. Tevelev, Stable pair, tropical, and log canonical compactifications of moduli spaces of del Pezzo surfaces, *Invent. Math.* 178 (2009) 173–227.
- [12] S. Herrmann, A. Jensen, M. Joswig, B. Sturmfels, How to draw tropical planes, *Electron. J. Combin.* 16 (2) (2009) R6.
- [13] A. Jensen, Gfan, a software system for Gröbner fans and tropical varieties, available at <http://home.imf.au.dk/jensen/software/gfan/gfan.html>.
- [14] S. Keel, Intersection theory of moduli space of stable n -pointed curves of genus zero, *Trans. Amer. Math. Soc.* 330 (2) (1992) 545–574.
- [15] D. Maclagan, B. Sturmfels, Introduction to Tropical Geometry, *Grad. Stud. Math.*, vol. 161, American Mathematical Society, 2015.
- [16] G. Mikhalkin, Tropical geometry and its applications, in: *International Congress of Mathematicians. Vol. II*, European Mathematical Society, Zürich, 2006, pp. 827–852.
- [17] G. Mikhalkin, J. Rau, Tropical geometry, in preparation, preliminary version available at <https://www.dropbox.com/s/g3ehtsoyy3tzkki/main.pdf>.
- [18] I. Naruki, Cross ratio variety as a moduli space of cubic surfaces, *Proc. Lond. Math. Soc.* (3) 45 (1) (1982) 1–30.
- [19] Q. Ren, S. Sam, G. Schrader, B. Sturmfels, The universal Kummer threefold, *Exp. Math.* 22 (2013) 327–362.
- [20] Q. Ren, S. Sam, B. Sturmfels, Tropicalization of classical moduli spaces, *Math. Comput. Sci., Special Issue on Computational Algebraic Geometry* 8 (2014) 119–145.

- [21] F. Rincon, Computing tropical linear spaces, *J. Symbolic Comput.* 51 (2013) 86–98.
- [22] B. Segre, *The Non-Singular Cubic Surfaces. A New Method of Investigation with Special Reference to Questions of Reality*, Oxford University Press, London, 1942.
- [23] K. Shaw, A tropical intersection product on matroidal fans, *SIAM J. Discrete Math.* 27 (2013) 459–491.
- [24] W.A. Stein, et al., *Sage Mathematics Software (Version 5.9)*, The Sage Development Team, 2013, <http://www.sagemath.org>.
- [25] M. Stillman, D. Testa, M. Velasco, Gröbner bases, monomial group actions, and the Cox rings of del Pezzo surfaces, *J. Algebra* 316 (2) (2007) 777–801.
- [26] B. Sturmfels, Z. Xu, Sagbi bases of Cox–Nagata rings, *J. Eur. Math. Soc. (JEMS)* 12 (2010) 429–459.
- [27] M. Vigeland, Smooth tropical surfaces with infinitely many tropical lines, *Ark. Mat.* 48 (2010) 177–206.